ORNL/TM-10916

OAK RIDGE NATIONAL LABORATORY

MARTIN MARIETTA

Robust Control Technique for Nuclear Power Plants

G. V. Murphy
J. M. Bailey

OAK RIDGE NATIONAL LABORATORY
CENTRAL RESEARCH LIBRARY
CIRCULATION SECTION
4500N ROOM 175
LIBRARY LOAN COPY
DO NOT TRANSFER TO ANOTHER PERSON
If you wish someone else to see this report, send in name with report and the library will arrange a loan.

OPERATED BY
MARTIN MARIETTA ENERGY SYSTEMS, INC.
FOR THE UNITED STATES
DEPARTMENT OF ENERGY

Printed in the United States of America. Available from
National Technical Information Service
U.S. Department of Commerce
5285 Port Royal Road, Springfield, Virginia 22161
NTIS price codes—Printed Copy: A05 Microfiche A01

This report was prepared as an account of work sponsored by an agency of the United States Government. Neither the United States Government nor any agency thereof, nor any of their employees, makes any warranty, express or implied, or assumes any legal liability or responsibility for the accuracy, completeness, or usefulness of any information, apparatus, product, or process disclosed, or represents that its use would not infringe privately owned rights. Reference herein to any specific commercial product, process, or service by trade name, trademark, manufacturer, or otherwise, does not necessarily constitute or imply its endorsement, recommendation, or favoring by the United States Government or any agency thereof. The views and opinions of authors expressed herein do not necessarily state or reflect those of the United States Government or any agency thereof.

ORNL/TM-10916
UC-530

Instrumentation and Controls Division

ROBUST CONTROL TECHNIQUE FOR NUCLEAR POWER PLANTS

G. V. Murphy*
J. M. Bailey*

Date Published: March 1989

*The University of Tennessee, Knoxville.

Prepared by the
OAK RIDGE NATIONAL LABORATORY
Oak Ridge, Tennessee 37831
operated by
MARTIN MARIETTA ENERGY SYSTEMS, INC.
for the
U.S. DEPARTMENT OF ENERGY
under Contact No. DE-AC05-84OR21400

MARTIN MARIETTA ENERGY SYSTEMS LIBRARIES

3 4456 0289429 6

CONTENTS

LIST OF FIGURES v

LIST OF TABLES vii

ABSTRACT ix

1. ROBUSTNESS OF FEEDBACK CONTROL SYSTEMS 1

1.1 INTRODUCTION 1
1.2 DEFINITION OF ROBUSTNESS 1

2. ROBUSTNESS CONCEPTS OF THE LQG AND LQG/LTR CONTROL SYSTEMS 3

3. RETURN RATIO, RETURN DIFFERENCE, AND INVERSE RETURN DIFFERENCE 5

4. REVIEW OF OPTIMAL CONTROL THEORY 6

4.1 INTRODUCTION 6
4.2 LINEAR QUADRATIC REGULATOR (LQR) 6
4.3 KALMAN FILTER 8

5. RETURN RATIOS FOR THE FULL-STATE AND OBSERVER-BASED FEEDBACK SYSTEMS 11

5.1 FULL-STATE FEEDBACK RETURN RATIO 11
5.2 OBSERVER-BASED FEEDBACK RETURN RATIO 12

6. OBTAINING ROBUSTNESS PROPERTIES AT THE INPUT TO AN OBSERVER-BASED FEEDBACK CONTROL SYSTEM 15

7. LQG/LTR DESIGN AT THE PLANT INPUT USING SINGULAR VALUES 18

7.1 THE LQR DESIGN STEP 18
7.1.1 Command Tracking and Disturbance Rejection 18
7.1.2 Robustness at the Plant Input 19

7.2 LOOP TRANSFER RECOVERY USING THE KALMAN FILTER 20

8. SENSITIVITY OF MULTIVARIABLE FEEDBACK SYSTEMS 21

8.1 DERIVATION OF THE MATRIX SENSITIVITY FUNCTION 21
8.2 SENSITIVITY COMPARISON CRITERIA 24

9. CONTROLLER DESIGN FOR THE DEAERATOR 26

9.1 THE LINEARIZED MODEL 26
9.2 LQG CONTROLLER DESIGN 28

9.3 LQG/LTR CONTROLLER DESIGN 29
9.4 PI CONTROLLER DESIGN 32
9.5 PRECOMPENSATOR DESIGN 34
9.6 ANALYSIS OF SINGULAR-VALUE PLOTS 39
9.6.1 PI Control System Singular-Value Plots 39
9.6.2 LQG Control System Singular-Value Plots 41
9.6.3 LQG/LTR Control System Singular-Value Plots 43

9.7 DEAERATOR STUDY SUMMARY AND CONCLUSIONS 43
9.7.1 Summary of Control System Analysis 43
9.7.2 Conclusions 44

REFERENCES 46

Appendix A. Singular Value Requirements for System Design 47

Appendix B. Classical Design of the Deaerator Control System . . . 53

Appendix C. Concepts of Eigenvectors, Vector Norms, Matrix . . . .
Norms, and Singular Values 63

LIST OF FIGURES

Figure		Page
2.1.	Summary block diagram of the robustness properties of the LQG	4
2.2.	Unity feedback model-based compensator (UFMBC)	4
3.1.	General block diagram	5
5.1.	Full-state feedback	12
5.2.	Observer-based feedback	13
8.1.	Block diagram of open-loop compensated system	21
8.2.	Unity feedback MIMO control system	22
9.1.	General process flow diagram of the deaerator	27
9.2.	LQG block diagram	28
9.3.	Alternate compensator structure	29
9.4.	Open-loop frequency response of the LQG control system	30
9.5.	Open-loop frequency response of the LQG/LTR control system	32
9.6.	Block diagram of PI control system	33
9.7.	Open-loop frequency response of PI control system	35
9.8.	PI control system closed-loop transient response	37
9.9.	LQG control system closed-loop transient response	38
9.10.	LQG/LTR control system closed-loop transient response	39
9.11.	LQG/LTR control system design closed-loop transient response with precompensator	40
9.12.	Plots of singular-value return ratio	41
9.13.	Plots of singular-value return difference	42
9.14.	Plots of singular-value inverse return difference	42
A1.	Unity feedback MIMO control system	50

LIST OF FIGURES (continued)

Figure		Page
B1.	General process flow diagram of the deaerator	55
B2.	Block diagram of the linearized system	57
B3.	Linearized system with unity feedback	57
B4.	Inner loop root locus	58
B5.	Outer loop root locus	59
B6.	Frequency response of inner loop	60
B7.	Open-loop frequency response of PI control system	61

LIST OF TABLES

Table		Page
1.	Deaerator poles and zeros	27
2.	LQG controller and deaerator poles and zeros	35
3.	LQG/LTR controller and deaerator poles and zeros	36
4.	PI controller and deaerator poles and zeros	36
5.	System design specifications	44
6.	Performance and robustness results	45

ABSTRACT

This report summarizes the linear quadratic Guassian (LQG) design technique with loop transfer recovery (LQG/LTR) for design of control systems. The concepts of return ratio, return difference, inverse return difference, and singular values are summarized.

The LQG/LTR design technique allows the synthesis of a robust control system. To illustrate the LQG/LTR technique, a linearized model of a simple process has been chosen. The process has three state variables, one input, and one output. Three control system design methods are compared: LQG, LQG/LTR, and a proportional plus integral controller (PI).

1. ROBUSTNESS OF FEEDBACK CONTROL SYSTEMS

1.1 INTRODUCTION

The advanced control strategies development group at Oak Ridge National Laboratory, has been actively engaged in exploring the applications of optimum control theory. Since October 1987, this effort has focused on robust control theory. One of the primary attractions of this theory is that it generalizes the single input-single output (SISO) concept of gain and phase margin and its effect on system sensitivity to a multivariable control system.

The purpose of this report is to summarize the derivation of a design technique based on robust control theory and to illustrate this technique by a model chosen for its simple structure.

1.2 DEFINITION OF ROBUSTNESS

A system is considered to be robust and have good robustness properties if it has a large stability margin, good disturbance attenuation, and/or low sensitivity to parameter variations.[1] The term "stability margin" refers to the gain margin and the phase margin, which are quantitative measures of stability. A proven method of obtaining good robustness properties is the use of a feedback control system, which can be designed to allow for variations in the system dynamics. Some causes of variation in system dynamics are as follows:

- modeling and data errors in the nominal plant and system;
- changes in environmental conditions, manufacturing tolerances, wear due to aging, and noncritical material failures; and
- errors due to calibration, installation, and adjustments.

Feedback control systems with good feedback properties have been synthesized for SISO systems. Classical frequency domain techniques such as Nyquist, root-locus, Bode, and Nichols plots have been used to obtain the feedback control system for the SISO system. These design techniques have allowed the synthesis of feedback control systems yielding insensitivity to bounded parameter variations and a large stability margin. The success of the feedback control system for the SISO system has led to the direct extension of the classical frequency domain technique to the design of a multivariable feedback control system. This extension to the multivariable design problem examines an individual feedback loop as the phase and gain margins are varied, while the nominal phase and gain values in the remaining feedback paths are held constant. This technique, however, fails to consider the results of simultaneous variation of gain and phase in all paths, which is a real-world possibility and needs to be considered. A method of obtaining a feedback control system with good robustness properties that

takes into consideration simultaneous gain and phase variation is the linear quadratic Guassian (LQG)[2] technique with loop transfer recovery (LQG/LTR).[3]

The LQG/LTR technique can be applied to multivariable input-multivariable output (MIMO) systems or SISO systems. The LQG/LTR technique not only has the good robustness properties of the classical frequency domain techniques but also is capable of minimizing the effects of unmodeled high-frequency dynamics, neglected nonlinearities, and a reduced-order model. A tool used in synthesizing the LQG/LTR technique is the computer-aided systems and control analysis and design environment (CASCADE),[4] an expert computer design tool that eliminates the numerical programming burden of programming the complex LQG/LTR algorithm. The CASCADE expert system was developed for the U.S. Department of Energy by the University of Tennessee at Knoxville.

In this report, some concepts will be defined and the LQG/LTR procedure for development of a model-based compensator (MBC) will be described. A unity-feedback MBC is selected for the controller, because of its similarity to the SISO unity-feedback control system well known to classical control designers. The MBC closed-loop control system has proven to offer great practical considerations in the design of automatic control systems.

2. ROBUSTNESS CONCEPTS OF THE LQG AND LQG/LTR CONTROL SYSTEMS

The LQG/LTR[5] design procedure is based on the system configuration of the LQG controller shown in Fig. 2.1. The LQG controller consists of a Kalman filter state estimator and a linear quadratic regulator. The Kalman filter state estimator has been shown to have good robustness properties for plant perturbations at the plant output. The linear quadratic regulator (LQR) has been shown to have good robustness properties for perturbations at the plant input. Even though its components separately have good robustness properties, however, the LQG controller is found to have no guaranteed robustness properties at either the input (point 2) or the output (point 3) of the plant.

The LQG/LTR design procedure allows us to recover robustness properties at either the input or the output of the plant. If robustness is desired at the input to the plant, first a nominal robust LQR design is made to satisfy the design constraints. Next, an LTR step is made to design a Kalman filter gain that recovers the robustness at the input to the plant of the LQG controller that is approximately that of the nominal LQR design. This implies from Fig. 2.1 that the robustness properties at points 1 and 2 are approximately the same.

If robustness is desired at the output of the plant, first a nominal robust Kalman filter design is made to satisfy the performance constraints. Next, an LTR step is made to design a LQR gain that recovers the robustness at the output of the plant that is approximately that of the nominal Kalman filter design. This implies from Fig. 2.1 that the robustness properties at points 3 and 4 are approximately the same.

The block diagram of the unity-feedback MBC is shown in Fig. 2.2. This control system structure will allow tracking and regulation of a reference input at the output of the plant. The filter and regulator gains used in the controller $K(s)$ are obtained appropriately, depending on whether robustness is desired at the input or the output of the plant. Note that the robustness properties of the unity-feedback MBC (UFMBC) are the same as those of the LQG system, since the UFMBC is just an alternate structure of the LQG system.

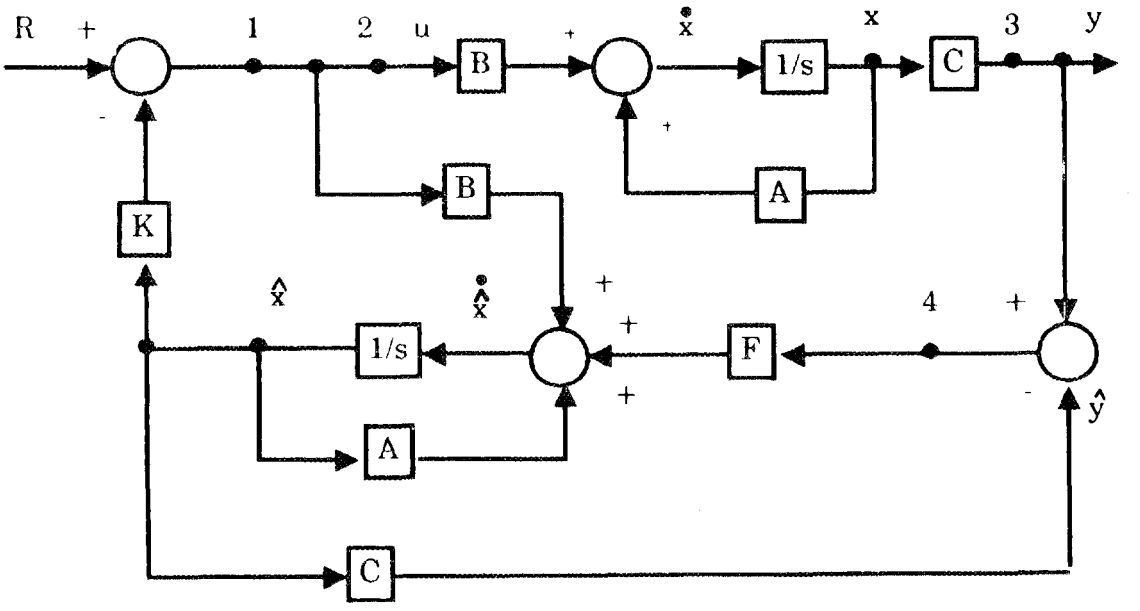

- LQG guaranteed no robustness properties at the input or output of the plant.
- Point 1 has the good robustness properties of the full-state feedback system.
- Point 4 has the good robustness properties of the Kalman filter.
- Point 2 has no guaranteed robustness properties.
- Point 3 has no guaranteed robustness properties.
- the LQG/LTR design method permits recovery of the robustness properties of point 1 at point 2 or the robustness properties of point 4 at point 3.

Fig. 2.1. Summary of the robustness properties of the LQG block diagram.

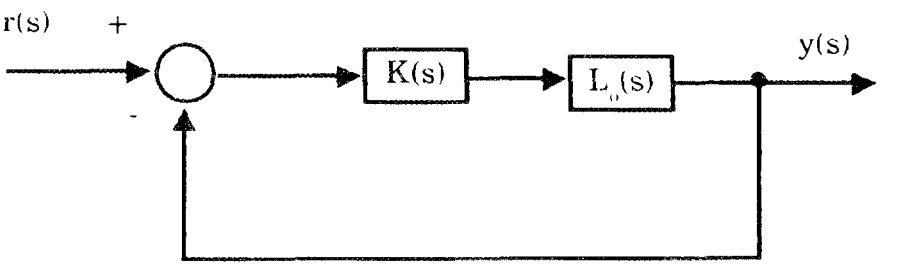

Fig. 2.2. Unity feedback model based compensator (UFMBC).

3. RETURN RATIO, RETURN DIFFERENCE, AND INVERSE RETURN DIFFERENCE

Throughout the literature on the LQG/LTR design procedure, the terms return ratio, return difference, and inverse return difference are frequently used. A simple explanation by example of these terms will be presented. Given the block diagram in Fig. 3.1, let us break the path at the input to the plant. Now take a path through the plant transfer function and follow the feedback path to the other side of the break. The multiplication of the transfer functions encountered in this path is defined as the return ratio. In this case the return ratio is $L_o(s)$.

From the block diagram the following transfer function can be obtained:

$$\frac{e(s)}{u(s)} = \frac{1}{I + L_o(s)} = (I + L_o(s))^{-1} \tag{3.1}$$

where I is the identity matrix and $I + L_o(s)$ is defined as the return difference. In this example the return difference can be used to characterize the error behavior in the system. From Fig. 3.1 also, the following closed-loop transfer function can be defined:

$$\frac{y(s)}{u(s)} = \frac{L_o(s)}{I + L_o(s)} = (I + L_o^{-1}(s))^{-1} \tag{3.2}$$

where $I + L_o^{-1}(s)$ is defined as the inverse return difference. Thus, using the properties of the inverse return difference, the closed-loop system can be examined.

The concepts defined above can be also applied to the block diagram of the LQG design. The details of obtaining the return ratio, return difference, and inverse return difference for consideration in the LQG/LTR procedure have been well documented in papers on the LQG/LTR design concept.[3] In this report, these terms will be referred to in relation to the requirements for the LQG/LTR design.

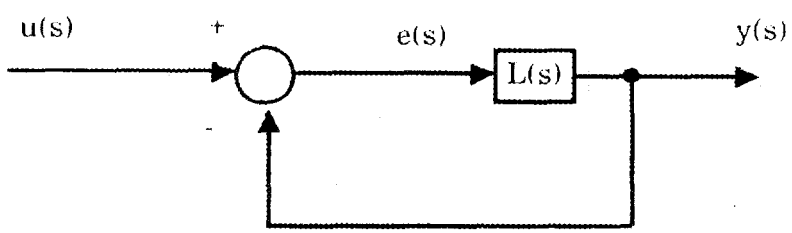

Fig. 3.1. General block diagram of plant with unity feedback.

4. REVIEW OF OPTIMAL CONTROL THEORY

4.1 INTRODUCTION

In the following sections the linear quadratic regulator based and the Kalman filter based optimal control problems will be reviewed briefly.[5] This review will be approached in a manner to set the framework for the study of the LQG and LQG/LTR control system designs.

4.2 LINEAR QUADRATIC REGULATOR (LQR)

Consider the linear time-invariant state-space system

$$\dot{x}(t) = Ax(t) + Bu(t) \quad . \tag{4.1}$$

where

$$y(t) = Cx(t) \quad . \tag{4.2}$$

The goal of this problem is to minimize the performance index

$$J = \int_0^\infty [x^T(t)Qx(t) + u^T(t)Ru(t)]dt + x^T(\infty)Zx(\infty) \tag{4.3}$$

where

$$\int_0^\infty x^T(t)Qx(t)dt = \text{integral square regulating error} \tag{4.4}$$

$$\int_0^\infty u^T(t)Ru(t)dt = \text{integral square input} \tag{4.5}$$

and

$$x^T(\infty)Zx(\infty) = \text{weighted square terminal error.} \tag{4.6}$$

The performance index J, referred to as the quadratic performance index, implies that a control $u(t)$ is sought to facilitate the minimization of J. The weighting matrices Q and R are selected to reflect the importance of particular states and control inputs. In general the weighting of the diagonal elements of Q can be determined by the importance of the state, as observed by the C matrix of the output equation. The effect of Q is the capability to control the transient response of the LQR. The effect of R is to control the energy resulting from u.

A necessary requirement to minimize J is that J is certainly finite. The condition that allows J to become infinite is that uncontrollable, unstable state trajectories appear in the performance index J. Thus the state-space system [A,B] must be completely controllable, and [A,B] must be stabilizable to ensure that the performance index is finite.

The control u for the optimization criteria for the steady state linear control law takes the form

$$u(t) = -Kx(t) \tag{4.7}$$

and differentiating Eq. (4.3), it can be shown that S is the solution of the steady state algebraic Riccati equation

$$\dot{S} = 0 = Q - SBR^{-1}B^{T}S + A^{T}S + SA \tag{4.8}$$

which yields a minimum for the performance index, where S, Q, and R are constant positive-definite symmetric matrices,

$$K = R^{-1}B^{T}S \tag{4.9}$$

At this point our problem of stabilizing the state trajectories appears to be complete, but this is not so. What happens when we do not account for unobserved and unstable state trajectories in the performance index of the optimal control law? The result is that the linear controller will not act on the unstable states, thus yielding a finite performance index but an unstable closed-loop system. To eliminate this potential problem, we must required Q to be positive definite, or $Q > 0$. Then the linear control law will yield an asymptotically stable system. Q can be allowed to be only positive semidefinite only if [A,C] is observable, where C is a matrix such that $Q = C^{T}C$ or $C = \sqrt{Q}$. Using

$$Q = C^{T}C \tag{4.10}$$

then

$$\begin{aligned} J &= \int_0^\infty [x^{T}Qx + u^{T}Ru]\,dt \\ &= \int_0^\infty [x^{T}C^{T}Cx + u^{T}Ru]\,dt \\ &= \int_0^\infty [y^{T}y + u^{T}Ru]\,dt \end{aligned} \tag{4.11}$$

which implies that the output system responses are being regulated.

As stated previously, the observability requirement of the pair [A,C] results in a sufficient condition for asymptotic stability of the closed-loop system. This can be made a necessary and sufficient condition by requiring the detectability of the pair [A,C], since only the unstable modes must be moved. Considering the restriction of detectability, the requirement that S be positive definite can be loosened to positive semidefinite.

Using the relaxed conditions, the following summary can be made regarding the linear quadratic regulator (LQR) problem. Given the linear time-invariant plant

$$\dot{x}(t) = Ax(t) + Bu(t) \tag{4.12}$$

which is stabilizable and controllable, then a finite performance index

$$J = \int_0^\infty [x^T(t)Qx(t) + u^T(t)Ru(t)]dt \tag{4.13}$$

exists, where Q is a symmetric positive semidefinite matrix and R is positive definite. Therefore a linear control law that minimizes J is defined as

$$u(t) = -Kx(t) \tag{4.14}$$

where

$$K = R^{-1}B^TS \tag{4.15}$$

where, in turn, S is a constant symmetric positive semidefinite matrix that satisfies the algebraic Ricatti equation

$$Q - SBR^{-1}B^TS + A^TS + SA = 0 \quad . \tag{4.16}$$

The closed loop regulator is given by

$$\dot{x}(t) = [A - BK]x(t) = [A - BR^{-1}B^TS]x(t) \tag{4.17}$$

and is asymptotically stable provided the state equation (4.1) and the output equation (4.2) are detectable.

4.3 KALMAN FILTER

Now we will examine a method of reconstructing an estimate of the states using only the output measurements of the system. The method of reconstruction must be applicable when process noise and measurement noise, respectively, corrupt the plant state equations and the output measurement equations.

Let us consider the stochastic linear system

$$\dot{x}(t) = Ax(t) + Bu(t) + \Gamma d(t) \tag{4.18}$$

$$y(t) = Cx(t) + n(t) \tag{4.19}$$

where $d(t)$ is a process noise random vector and $n(t)$ is a measurement noise random vector. Assuming that $d(t)$ and $n(t)$ are zero-mean, uncorrelated, Guassian white noises, therefore

$$E[d(t)]E[n(t)] = 0 \qquad \text{for all } t \tag{4.20}$$

$$E[d(t)d^T(\tau)] = D_o\delta(t - \tau) \tag{4.21}$$

$$E[n(t)n^T(\tau)] = N\delta(t - \tau) \qquad \text{for all } t < \tau \tag{4.22}$$

$$E[d(t)n^T(\tau)] = 0 \tag{4.23}$$

where N and D_o are constant symmetric, positive definite and positive semi-definite matrices, respectively. Note that N and D_o are constant because it is assumed that $d(t)$ and $n(t)$ are wide-sense stationary.

The state estimate $\hat{x}$ of the state x is obtained from the noisy measurement y. Therefore we can define a state error vector

$$e(t) = x(t) - \hat{x}(t) \tag{4.24}$$

where we desire to minimize the mean square error

$$\bar{e} = E[e^T(t)e(t)] \quad . \tag{4.25}$$

The estimator can thus be shown to take the form

$$\dot{\hat{x}} = A\hat{x}(t) + Bu(t) + F[y(t) - Cx(t)] \tag{4.26}$$

where F is the filter gain which minimizes Eq. (4.25); F is defined as

$$F = \Sigma C^T N^{-1} \tag{4.27}$$

where Σ is constant variance matrix of the error $e(t)$. It is assumed here that $e(t)$ is wide-sense stationary. The Σ is obtained by solving the algebraic variance Riccati equation

$$D - \Sigma C^T N^{-1} C\Sigma + A\Sigma + \Sigma A^T = 0 \tag{4.28}$$

where

$$D = \Gamma D_o \Gamma^T \quad . \tag{4.29}$$

A sufficient condition to obtain a unique and positive definite Σ from Eq. (4.28) requires that [A,C] be completely observable. However if the pair [A,C] is required to be detectable then Σ can be positive semidefinite.

The reconstruction error $e(t)$ satisfies the differential equation

$$\dot{e}(t) = [A - FC]e(t) + [\Gamma \quad -F] \begin{bmatrix} d(t) \\ n(t) \end{bmatrix} \tag{4.30}$$

such that

$$e(t) \to 0 \quad \text{as} t \to \infty \quad \forall t \geq t_o$$

if and only if the observer is asymptotically stable. The poles of the observer (filter) are found using the closed-loop dynamics matrix $[A-FC]$. To obtain asymptotic stability of the filter, it is required that the pair $[A,\Gamma]$ be completely controllable. The necessary and sufficient condition of stabilizability of the pair $[A,\Gamma]$ will ensure stability also.

5. RETURN RATIOS FOR THE FULL-STATE AND OBSERVER-BASED FEEDBACK SYSTEMS

5.1 FULL-STATE FEEDBACK RETURN RATIO

For the full-state feedback system of Fig. 5.1 with no loops broken, it can be stated[5] that

$$x = \Phi B u = \Phi B u' \tag{5.1}$$

and

$$u = R - Kx \quad . \tag{5.2}$$

Substituting Eq. (5.1) into Eq. (5.2) and solving for u yields

$$u = (I + K\,\Phi B)^{-1} R \quad , \tag{5.3}$$

thus

$$x = \Phi B (I + K\Phi B)^{-1} R \quad . \tag{5.4}$$

Now let us examine the loop transfer function from control signal u' to control signal broken at point 1, assuming that $R = 0$. For this full-state feedback case it follows that

$$x = \Phi B u' \tag{5.5}$$

and

$$u = -Kx \quad . \tag{5.6}$$

Substituting Eq. (5.5) into Eq. (5.6) yields

$$u = -K\Phi B u' \quad . \tag{5.7}$$

Finally, for the full-state feedback system, find the loop transfer function from control signal u" when the loop is broken at point 2. In this case it follows that, with $R = 0$,

$$x = \Phi B u'' \tag{5.8}$$

and

$$u = u' = -Kx \quad . \tag{5.9}$$

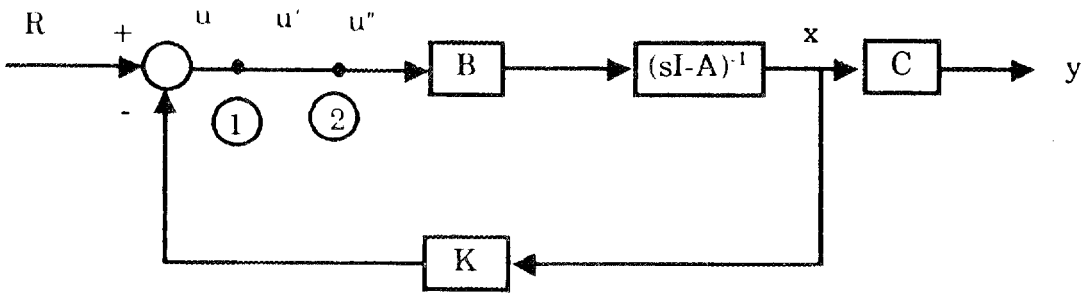

Fig. 5.1. Full state feedback.

Substituting Eq. (5.8) into Eq. (5.9) yields

$$u = u' = -K\Phi Bu'' \quad . \tag{5.10}$$

5.2 OBSERVER-BASED FEEDBACK RETURN RATIO

For the observer-based feedback system of Fig. 5.2 with no loops broken, it follows[6] that

$$x = \Phi Bu = \Phi Bu' = \Phi Bu'' \quad . \tag{5.11}$$

and

$$y = Cx \quad . \tag{5.12}$$

Now substituting Eq. (5.12) and Eq. (5.11) into

$$\hat{x} = \Phi[Bu' + Fy - FC\hat{x}]$$

results in

$$\begin{aligned} \hat{x} &= \Phi[Bu' + FCx - FC\hat{x}] \\ \hat{x} &= \Phi[Bu' + FC\Phi Bu' - FC\hat{x}] \\ \hat{x} &= \Phi[Bu' + FC\Phi Bu'] - \Phi FC\hat{x} \end{aligned} \tag{5.13}$$

thus

$$\hat{x} = (I + \Phi FC)^{-1}\Phi(B + FC\Phi B)u' \tag{5.14}$$

which simplifies to

$$\hat{x} = \Phi Bu' \quad . \tag{5.15}$$

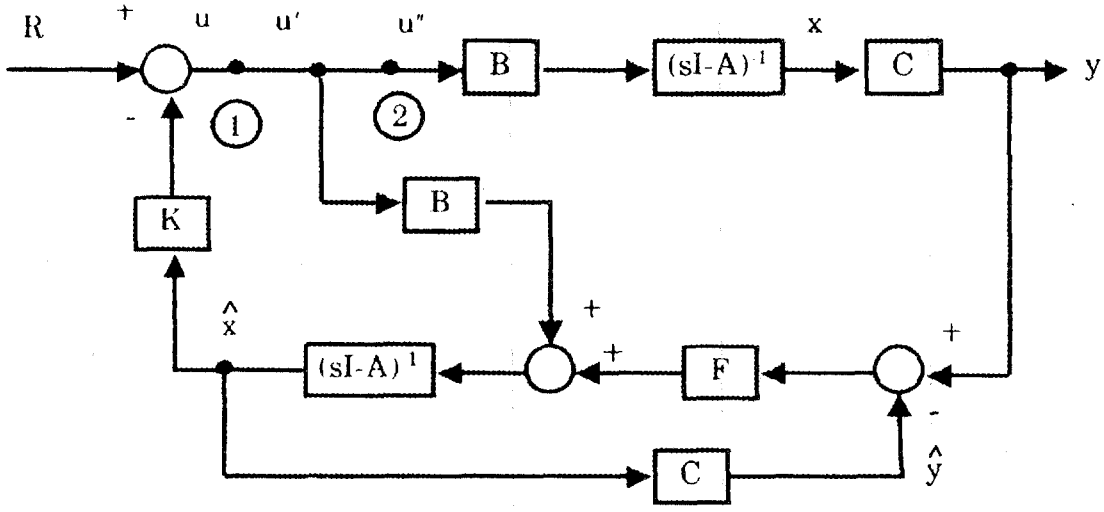

Fig. 5.2. Observer-based feedback.

Now examining the control u, it follows that

$$u = R - K\hat{x} \tag{5.16}$$

and substituting Eq. (5.15) into Eq. (5.16) results in

$$u = R - K\Phi Bu \quad . \tag{5.17}$$

The control u can thus be defined as

$$u = (I + K\Phi B)^{-1}R \tag{5.18}$$

Substituting Eq. (5.18) into Eq. (5.11) results in

$$x = \Phi B(I + K\Phi B)^{-1}R \tag{5.19}$$

which is the same as the result for the full state feedback system.

Now let us find the loop transfer function from control signal u' to control signal u when the loop is broken at point 1 of the observer-based feedback system. It follows that

$$u = -K\hat{x} \tag{5.20}$$

and substituting Eq. (5.15) into Eq. (5.20) yields

$$u = -K\Phi Bu' \quad . \tag{5.21}$$

In this case it is clear that $u' = u''$. Also note that the result of Eq. (5.21) is the same as the result found in the full state feedback case.

Finally, for this observer-based feedback system, the loop transfer function from control signal u'' to control signal u' when the loop is broken at point 2 will be found. For this case

$$\hat{x} = \Phi(Bu' + FC\Phi Bu'') - \Phi FC\hat{x} \tag{5.22}$$

and solving for $\hat{x}$ results in

$$\hat{x} = (I + \Phi FC)^{-1}\Phi(Bu' + FC\Phi Bu'') \quad . \tag{5.23}$$

Further simplification of Eq. (5.23) results in

$$\hat{x} = \Phi[B(C\Phi B)^{-1} - F(I + C\Phi F)^{-1}]C\Phi Bu' + \Phi[F(I + C\Phi F)^{-1}]C\Phi Bu'' \tag{5.24}$$

where the plant in this case is square and invertible.

Now the control for this case is defined as

$$u = u' = -K\hat{x} \tag{5.25}$$

where $\hat{x}$ is defined in Eq. (5.24). This result implies that there is a difference between the control u obtained in Eq. (5.25) for the observer-based feedback system and the control u obtained for the full state feedback system.

From the examination of the loop transfer properties of the full state feedback system and the observer-based system, it is clear that the input of the observer-based system does not have the good robustness properties of the LQR system. What now is desirable is a means of approximating the loop properties of point 1 at point 2 of the observer-based system.

6. OBTAINING ROBUSTNESS PROPERTIES AT THE INPUT TO AN OBSERVER-BASED FEEDBACK CONTROL SYSTEM

From our previous examination of the observer-based feedback control system commonly referred to as the Linear Quadratic Guassian (LQG) control system there are no guaranteed robustness properties at the input to the plant (point 2 of Fig. 5.2). Now a method will be summarized that recovers the good robustness properties of the input (point 2) of the LQR at the input (point 2) of the LQG control system.

Provided that the regulator gain for the LQR has been selected, now a filter gain must be solved for in order to equate the control for the LQG control system for loop break at point 2, which is

$$u = -K\hat{x} \tag{6.1}$$

where

$$\hat{x} = \Phi[B(C\Phi B)^{-1} - F(I + C\Phi F)^{-1}]C\Phi Bu' + \Phi[F(I + C\Phi F)^{-1}]C\Phi Bu'' \tag{6.2}$$

to the control

$$u = -K\Phi Bu'' \tag{6.3}$$

of the LQR for a loop break at point 2.[6] To equate the control Eq. (6.1) to the control Eq. (6.3) requires that the following equation be satisfied:

$$B(C\Phi B)^{-1} = F(I + C\Phi F)^{-1} \quad . \tag{6.4}$$

Therefore an appropriate value of F must be found to satisfy Eq. (6.4).

Now to select a value of F, we will assume that F is a function of a scalar parameter q such that

$$\frac{F(q)}{q} \to BW \quad \text{as} \quad q \to \infty \tag{6.5}$$

where W is any nonsingular matrix. Therefore, using the right-hand sides of Eqs. (6.4) and (6.5), then

$$\begin{aligned} F(I + C\Phi F)^{-1} &= \frac{F(q)}{q}\, q[I + C\Phi F(q)]^{-1} \\ &= \frac{F(q)}{q}\left(\frac{I}{q} + C\Phi\,\frac{F(q)}{q}\right)^{-1} \end{aligned} \tag{6.6}$$

which implies that as $q \to \infty$ Eq. (6.6) becomes

$$BW(C\Phi BW)^{-1} = B(C\Phi B)^{-1} \quad , \tag{6.7}$$

which satisfies the equality requirements of Eq. (6.4) for $W = I$, an identity matrix.

As previously discussed, the error dynamics of the Kalman filter must be asymptotically stable. This requires that an appropriate error noise statistics $\Sigma(q)$ satisfies

$$0 = A\Sigma(q) + \Sigma(q)A^{T} + D(q) - \Sigma(q)C^{T}N^{-T}C\Sigma(q) \tag{6.8}$$

such that

$$F(q) = \Sigma(q)C^{T}N^{-1} \tag{6.9}$$

where $D(q)$ is a positive semidefinite and N is a positive definite, and $[A, D^{\frac{1}{2}}]$ and $[C, A]$ are respectively stabilizable and detectable.

Now $D(q)$ the process noise intensities and N the measurement noise intensities are to be respectively defined as

$$D(q) = \Gamma D_{o}\Gamma^{T} + q^{2}BVB^{T} \tag{6.10}$$

and

$$N = N_{o} \tag{6.11}$$

where $\Gamma = I$, $D_{o} = C^{T}C$, and V is any positive definite symmetric matrix.

Substituting Eqs. (6.10) and (6.11) into Eq. (6.8) results in

$$O = A\Sigma(q) + \Sigma(q)A^{T} + D_{o} + q^{2}BVB^{T} - \Sigma(q)C^{T}N_{o}^{-1}C\Sigma(q) \tag{6.12}$$

which implies that

$$O = A\frac{\Sigma(q)}{q^{2}} + \frac{\Sigma(q)A^{T}}{q^{2}} + \frac{D_{o}}{q^{2}} + BVB^{T} - \frac{\Sigma(q)}{q^{2}}q^{2}C^{T}N_{o}^{-1}C\frac{\Sigma(q)}{q^{2}} \quad . \tag{6.13}$$

Now let $q \to \infty$ in Eq. (6.13); thus

$$q^{2}\frac{\Sigma(q)}{q^{2}}C^{T}N_{o}^{-1}C\frac{\Sigma(q)}{q^{2}} \to BVB^{T} \tag{6.14}$$

and using Eq. (6.9), the left-hand side of Eq. (6.14) is then

$$\frac{F(q)N_oF(q)^T}{q^2} = q^2 \frac{\Sigma(q)}{q^2} C^T N_o^{-1} C \frac{\Sigma(q)}{q^2} \quad , \tag{6.15}$$

which implies that as $q \to \infty$

$$\frac{F(q)N_oF(q)^T}{q^2} \to BVB^T \quad , \tag{6.16}$$

thus

$$\frac{F(q)}{q} \to BV^{\frac{1}{2}}N_o^{-\frac{1}{2}} \tag{6.17}$$

$$W = V^{\frac{1}{2}}N_o^{-\frac{1}{2}} \quad . \tag{6.18}$$

Thus it can be concluded that as $q \to \infty$ the loop properties at the input to the plant of the LQG control system approach the input properties of the LQR control system. Note, however, that as $q \to \infty$ the process noise intensity is seen to differ significantly from the assumed process noise. However, as $q \to 0$ the Kalman filter is approached. Thus when $q = 0$ the LQG system has no guaranteed loop properties at the input. It appears that a trade-off must be made between obtaining an accurate filter and obtaining good loop transfer properties.

7. LQG/LTR DESIGN AT THE PLANT INPUT USING SINGULAR VALUES

7.1 THE LQR DESIGN STEP

Now the LQR design step of the LQG/LTR design procedure will be summarized using the singular-value concept (see Appendix C). First, the Kalman equality for the LQR is defined as

$$\begin{aligned}[I + K(sI - A)^{-1}B]^*[I + K(sI - A)^{-1}B] \\ = I + \frac{1}{\rho}\,[B^T(sI - A^T)^{-1}P^TP(sI - A)^{-1}B] \\ = I + \frac{1}{\rho}[P(sI - A)^{-1}B]^*[P(sI - A)^{-1}B] \quad .\end{aligned} \tag{7.1}$$

where * indicates the complex conjugate transpose, $Q = P^TP$, and $R = \rho I$.

It then follows from Eq. (7.1) that

$$[I + L_2]^*[I + L_2] = I + \frac{1}{\rho}[P\Phi B]^*[P\Phi B] \tag{7.2}$$

where $L_2(s) = K\Phi B$ is the return ratio of the LQR at point 2 (see Fig. 5.1) and $\Phi = (sI - A)^{-1}$. Finding the eigenvalue of Eq. (7.2) results in

$$\lambda\{[I + L_2(s)]*[I + L_2(s)]\} = 1 + \frac{1}{\rho}\,\lambda[[P\Phi B]*[P\Phi B]] \tag{7.3}$$

thus it can be stated that system singular values are

$$\sigma_i[I + L_2(s)] = \sqrt{1 + \frac{1}{\rho}\,\sigma_i{}^2[P\Phi B]} \quad . \tag{7.4}$$

7.1.1 Command Tracking and Disturbance Rejection[6]

Assuming that command following and disturbance rejection will occur at low frequencies requires that at low frequencies

$$\sigma_{min}(L_2(s)) >> 1 \quad . \tag{7.5}$$

This condition results in Eq. (7.4) becoming

$$\sigma_{min}(L_2(s)) \approx \frac{1}{\sqrt{\rho}}\,\sigma_{min}\,(P\Phi B) \quad . \tag{7.6}$$

By using this approximation, the solution of the Riccati equation is avoided in computing $(L_2(s)$. This approximation therefore allows the plotting of the singular values of $L_2(s)$ for various values of ρ and P with minimum effort.

The value of P must be selected to balance the minimum and maximum singular values of $L_2(s)$ at either a low, a high, or an arbitrary frequency. The value of ρ has the effect of lowering or raising the singular-value plots, depending on the magnitude of ρ selected. An explanation of the relationship between the singular-value plots and the performance and robustness properties is given in Appendix A.

7.1.2 Robustness at the Plant Input[6]

It is assumed that the unstructured uncertainty takes the form of $\Delta L(s)$. This uncertainty is assumed to become significantly large at high frequencies. Considering that multiplicative perturbations are occurring at the input to the plant, to obtain good robustness properties requires that

$$\sigma_{\min}[I + L_2(s)^{-1}] > \|\Delta L(s)\| \quad . \tag{7.7}$$

Provided that $C\Phi B$ is minimum phase, the LQR gain becomes

$$\sqrt{\rho}K \rightarrow WP \tag{7.8}$$

as $\rho \rightarrow 0$. At high frequencies $j\omega$ can be defined as

$$s = \frac{jc}{\sqrt{\rho}} \tag{7.9}$$

as $\rho \rightarrow 0$, where c is constant. Therefore

$$L_2 \frac{jc}{\sqrt{\rho}} = K \frac{jc}{\sqrt{\rho}} I - A^{-1} B$$

$$= \sqrt{\rho}K(jcI - \sqrt{\rho}A)^{-1}B \tag{7.11}$$

Using Eq. (7.8) in Eq. (7.11) results in

$$L_2 \frac{jc}{\sqrt{\rho}} = \frac{\text{WPB}}{jc}, \text{ as } \rho \rightarrow 0 \quad . \tag{7.12}$$

The constant c can be defined as

$$c = \frac{\omega}{\sqrt{\rho}} \tag{7.13}$$

using $s = j\omega$ in Eq. (7.9). The maximum crossover frequency $w_{c_{max}}$ occurs where

$$\sigma_{\max}[L_2(jw_{c_{max}})] = \sigma_{\max} \frac{WPB}{j\omega_{c_{max}}\sqrt{\rho}} = 1 \tag{7.14}$$

and W is an orthonormal matrix.

$$\omega_{c_{max}} = \sigma_{max} \frac{PB}{\sqrt{\rho}} \tag{7.15}$$

where $\omega_{c_{max}}$ is less than the frequency at which

$$\|\Delta L(jw)\| = 1 \quad . \tag{7.16}$$

The system crossover frequency $\omega_{c_{max}}$ in Eq. (7.15) is only an approximate value.

7.2 LOOP TRANSFER RECOVERY USING THE KALMAN FILTER

Having designed the LQR to obtain good low-frequency performance specifications and robustness properties, the design of a Kalman filter to recover the robustness properties at the plant input of the LQG is considered.[6]

The open-loop plant $C\Phi B$ must be minimum phase, having an equal number of inputs and outputs or having more outputs than inputs.

If the system is nonsquare, then $C\Phi B$ and $F\Phi B$ must be augmented to become square. Next the Kalman filter is designed, using the following process and noise intensity matrices

$$D = \Gamma D_o \Gamma^T + q^2 BVB^T \tag{7.17}$$

$$N = \mu I \tag{7.18}$$

where q is a scalar and V is an arbitrary symmetric positive definite matrix, as discussed in Sect. 6. Now as $q^2 \to \infty$ the return ratio at point 2 of the observer-based system approaches $K\Phi B$, the return ratio at point 2 of the LQR system.

8. SENSITIVITY OF MULTIVARIABLE FEEDBACK SYSTEMS

8.1 DERIVATION OF THE MATRIX SENSITIVITY FUNCTION

In Sect. 7, the LQG/LTR concept was introduced. A design procedure was developed that produced command tracking, disturbance rejection, and robustness at the plant input. In this section, the linear sensitivity relationship between the closed-loop output error and the equivalent open-loop output error is derived. This sensitivity function takes the form of the inverse of the return difference matrix, discussed in Sect. 3. The importance of this sensitivity function is that it allows the synthesis of a multivariable closed-loop control system more insensitive to parameter variations in the plant than an equivalent open-loop system.[7]

As the first step in the design process, the Laplace transforms of some signals of the open-loop control system as shown in Fig. 8.1 are defined. The Laplace transforms are as follows:

$$Y_0(s) = L(s)U_0(s) \tag{8.1}$$

$$U_0(s) = K_1(s)R(s) \tag{8.2}$$

where $Y_0(s)$ is the output signal of the nominal plant $U_0(s)$ is the output signal of the open-loop compensator $K_1(s)$, $R(s)$ is the input signal of the open-loop control system, and L(s) is the Laplace transform of the nominal plant.

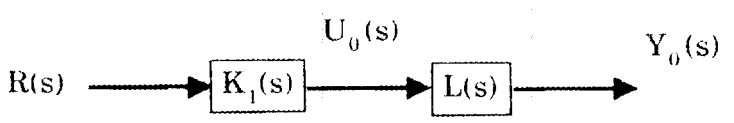

Fig. 8.1. Block diagram of open-loop compensated system.

In actual practice a plant will deviate from the nominal plant because of parameter variations. Let us define the perturbed plant transfer function as $L'(s)$; thus

$$Y_0'(s) = L'(s)U_0(s) \tag{8.3}$$

where $Y'_0(s)$ is the output that results when parameter variations of the plant occur. Therefore it can be stated that

$$E_0(s) = Y_0(s) - Y_0'(s) \tag{8.4}$$

where $E_0(s)$ is the Laplace transform of the error in the plant output signal when parameter variations in the nominal plant occur.

A closed-loop control system of the form shown in Fig. 8.2 is now examined. The Laplace transforms of the signals are defined as follows:

$$Y_c(s) = L(s)U_c(s) \tag{8.5}$$

$$U_c(s) = K(s)[R(s) - Y_c(s)] \tag{8.6}$$

where $Y_c(s)$, $U_c(s)$, and $K(s)$ are respectively the plant output, control input to the plant, and compensator of the closed-loop control system.

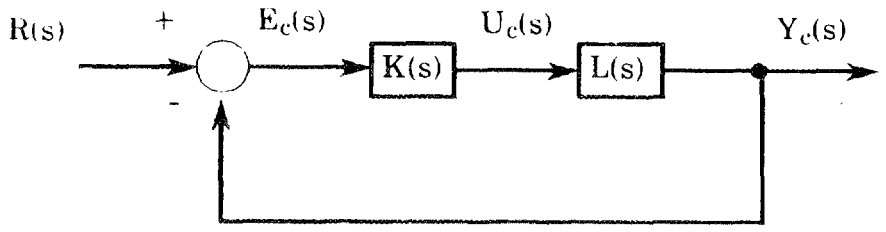

Fig. 8.2. Unity feedback MIMO control system.

Now define the signals resulting from parameter variations in the nominal plant of the closed-loop control system as follows:

$$Y_c'(s) = L'(s)U_c'(s) \tag{8.7}$$

$$U_c'(s) = K(s)[R(s) - Y_c'(s)] \tag{8.8}$$

The deviation of the output of the nominal system due to plant parameter variations is defined as

$$E_c(s) = Y_c(s) - Y_c'(s) \quad . \tag{8.9}$$

Substituting Eq. (8.6) into Eq. (8.5) and solving for $Y_c(s)$ yields

$$Y_c(s) = [I + L(s)K(s)]^{-1}L(s)K(s)R(s) \tag{8.10}$$

and, also, substituting Eq. (8.8) into Eq. (8.7) and solving for $Y_c(s)$ yields

$$Y_c'(s) = [I + L'(s)K(s)]^{-1}\, L'(s)K(s)R(s) \quad . \tag{8.11}$$

Therefore it follows that

$$E_c(s) = Y_c(s) - Y_c'(s) \tag{8.12}$$

can be rewritten as

$$\begin{aligned} E_c(s) = {} & [(I + L(s)K(s))^{-1}L(s)K(s) \\ & - (I + L'(s)K(s))^{-1}L'(s)K(s)R(s) \quad . \end{aligned} \tag{8.13}$$

Now define the term

$$\Delta L(s) = L'(s) - L(s) \tag{8.14}$$

which represents the error of the plant transfer function due to parameter variations. From this point on for simplicity we will suppress the use of the s in representing the Laplace transforms. Using Eq. (8.14), it follows that

$$L' = L + \Delta L \tag{8.15}$$

which is the perturbed plant transfer. Using Eq. (8.15) in Eq. (8.13) yields

$$\begin{aligned} E_c &= [(I + LK)^{-1}LK - (I + (L + \Delta L)K)^{-1}\ (L + \Delta L)K]R \\ &= (I + (L + \Delta L)K)^{-1}\ [(I + (L + \Delta L)K)(I + LK)^{-1}LK - (L + \Delta L)K]R \\ &= (I + (L + \Delta L)K)^{-1}\ [(I + (L + \Delta L)K)(I + LK)^{-1}LK - LK - \Delta LK]R \\ &= (I + (L + \Delta L)K)^{-1}\ [(\Delta LK(I + LK)^{-1}LK - \Delta LK]R \\ &= (I + (L + \Delta L)K)^{-1}\ [(\Delta LK(T - I)] \end{aligned} \tag{8.16}$$

where

$$T = (I + LK)^{-1}LK \quad . \tag{8.17}$$

From Eq. (8.10), it follows that

$$Y_c = TR \tag{8.18}$$

and recalling that the open-loop and closed-loop control systems have equivalent results implies that

$$Y_c = Y_0 \quad . \tag{8.19}$$

Considering that Eq. (8.19) holds, this further implies that

$$U_0 = U_c \tag{8.20}$$

then using Eqs. (8.6) and (8.18), Eq. (8.20) becomes

$$U_0 = U_c = K[I - T]R \quad . \tag{8.21}$$

Recall that

$$E_0 = (L - L')U_0 = -\Delta L U_0 = -\Delta LK[I - T]R$$

$$E_0 = \Delta LK[T - I]R \quad . \tag{8.22}$$

thus using Eq. (8.22) in Eq. (8.16), then Eq. (8.16) becomes

$$E_c = (I + (L + \Delta L)K)^{-1}E_0 \tag{8.23}$$

Now assuming that $L'K \approx LK$ for small parameter variations, then it follows that

$$E_c = (I + LK)^{-1}E_0 \tag{8.24}$$

where $I + LK$ is the return difference. Thus from the derivation of Eq. (8.24), the sensitivity function

$$S(s) = (I + LK)^{-1} \tag{8.25}$$

is obtained, which relates the closed-loop and open-loop errors.

8.2 SENSITIVITY COMPARISON CRITERIA

Now a performance index will be defined, to ensure that the closed-loop feedback system is less sensitive to parameter variations than an equivalent open-loop system. This performance index uses the integrated square of the error and takes the form

$$\text{Performance Index} = \int_0^{t_1} e^T(t)e(t)dt \tag{8.26}$$

where $e(t)$ can be the open-loop or closed-loop error and $t_1 > 0$. The value of t_1 is practically selected to be 4 or 5 times the largest "time constant" of the system. Thus, for the closed-loop system to be less sensitive than the open-loop system, the following inequality must be satisfied

$$\int_0^{t_1} e_c^T(t)e_c(t)dt < \int_0^{t_1} e_o^T(t)e_o(t)dt \quad . \tag{8.27}$$

The inequality of Eq. (8.27) results in a sufficient condition requiring the sensitivity matrix to satisfy

$$S^T(-j\omega)S(j\omega) - I \leq 0 \qquad \forall\omega\epsilon F \tag{8.28}$$

where F is the frequency band of interest.

The inequality given in Eq. (8.28) can be rewritten using singular values as follows:

$$\sigma_{\min}(S(s)) \gg 1 \quad \forall \omega \epsilon F \tag{8.29}$$

or

$$\sigma_{\min}(I + L(s)K(s)) \gg 1 \quad \forall \omega \epsilon F \tag{8.30}$$

The inequality of Eq. (8.30) can conflict with system design requirements of command/disturbance for the LQG/LTR control system design obtaining robustness at the plant output. It should be also noted that the resulting output sensitivity is fixed when robustness is obtained at the plant input. The only way to change the output sensitivity is by trail-and-error compromise and modification of the plant input design requirements.

9. CONTROLLER DESIGN FOR THE DEAERATOR

In this section, three linear control methods are used to obtain a level-control system design for a deaerator. The three linear control system design methods that will be used are proportional plus integral (PI), linear quadratic Gaussian (LQG), and linear quadratic Gaussian with loop transfer recovery (LQG/LTR). In this investigation, the dual of the procedure developed for the LQG/LTR design at the plant input will be used to obtain a robust control system design at the plant output.

The Bode gain and phase plots of the resulting control system design will be presented for each controller. Also, the singular-value plots of the return ratio, return difference, and inverse return difference for a break at the plant output will be presented.

The deaerator was chosen because of its simple mathematical structure; one input, one output, and three state variables. Thus the model easy to follow but complex enough to illustrate the design technique.

9.1 THE LINEARIZED MODEL

The mathematical model of the deaerator is nonlinear, with a process flow diagram as shown in Fig. 9.1. This nonlinear plant is linearized about a nominal operating condition. The resulting linearized plant model will be used to obtain the controller design. The linear deaerator model is described by

$$\dot{x}(t) = Ax(t) + Bu(t) \tag{9.1}$$

$$y(t) = Cx(t) \tag{9.2}$$

where A, B, and C are given respectively as

$$A = \begin{bmatrix} -53.802 & 1.7093 & 9.92677 \\ 1.761\text{E-}4 & -9.245\text{E-}04 & -0.0053004 \\ -0.001124 & -0.0243636 & -0.139365 \end{bmatrix}$$

$$B = \begin{bmatrix} -9526.25 \\ 0.265148 \\ -1.72463 \end{bmatrix}$$

and

$$C = [\ 0.0\ \ 3.2833\ \ 0.06373\ ] \quad .$$

The states are defined as

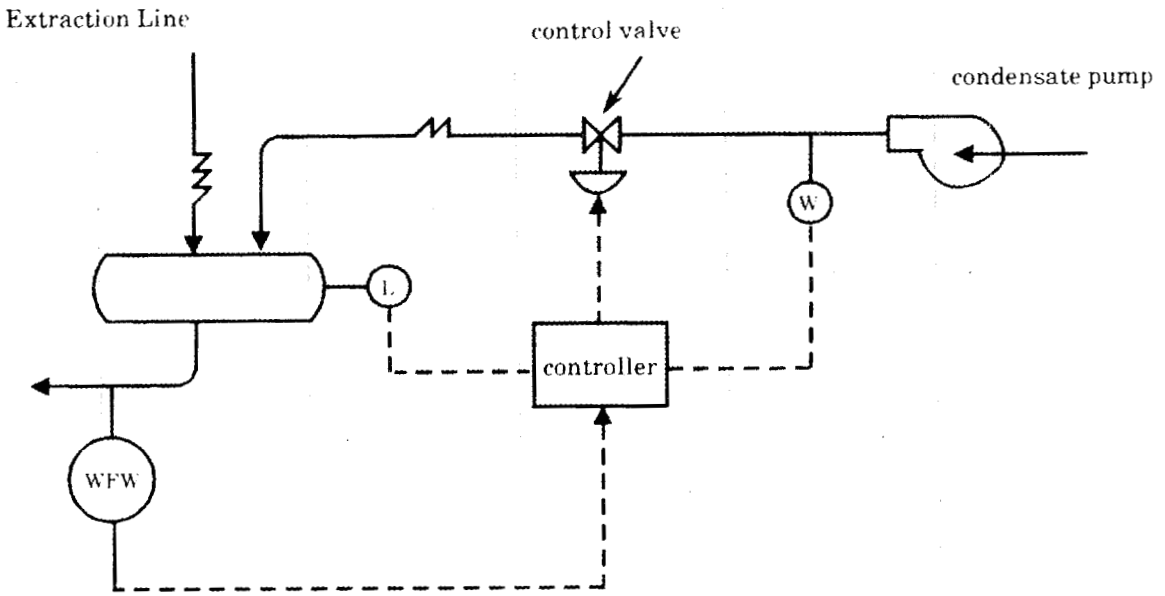

Fig. 9.1. General process flow diagram of the deaerator.

$$x = \begin{bmatrix} \delta P \\ \delta \rho \\ \delta H \end{bmatrix}$$

- δP – operating pressure between the pump and the extraction line
- $\delta \rho$ – fluid density
- δH – internal energy of the tank level

with an output

y = change in deaerator tank level

and plant input

u = change in control valve.

The poles and zeros of the deaerator model are shown in Table 1.

Table 1. Deaerator poles and zeros[a]

Poles		Zeros	
(1)	1.99E-06	(1)	−0.199
(2)	−0.141	(2)	−47.5
(3)	−53.8		

[a]Note: System gain = 0.76.

9.2 LQG CONTROLLER DESIGN

The design considerations for the tracking LQG control system will first be discussed. The block diagram of the LQG control system is shown in Fig. 9.2. It is apparent that output tracking of a reference input will not occur with the present LQG controller configuration. An alternate compensator structure, shown in Fig. 9.3, is therefore used to obtain a tracking LQG controller. The controller $C(s)$ uses the same filter gain (F) and regulator gain (K) as computed by the LQG design procedure.

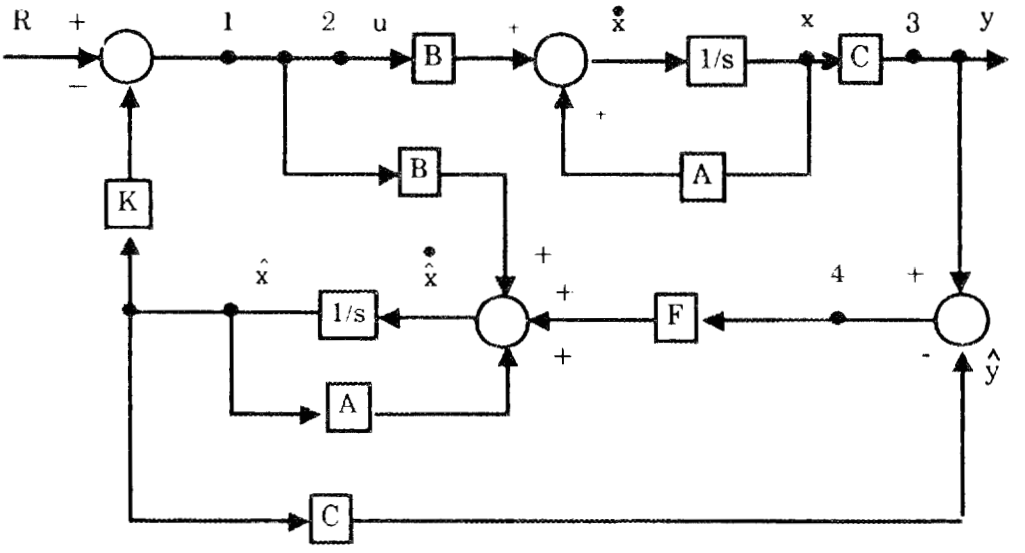

Fig. 9.2. LQG block diagram.

The regulator performance index is defined as

$$J = \int_0^\infty [x^T Q x + u^T R u] dt \tag{9.3}$$

where

$$Q = \begin{bmatrix} 0.005 & 0.0 & 0.0 \\ 0.0 & 100.0 & 0.0 \\ 0.0 & 0.0 & 1.0 \end{bmatrix}$$

and

$$R = 10^{-9} \quad .$$

The estimator is defined such that

$$\dot{x} = Ax + Bu + \Gamma d \tag{9.4}$$

$$y = Cx + n \tag{9.5}$$

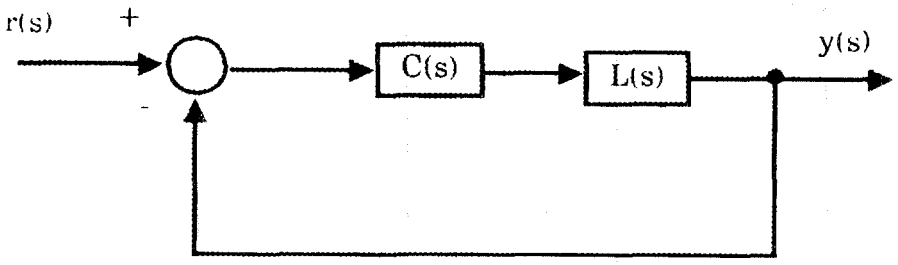

Fig. 9.3. Alternate compensator structure.

$$E[\Gamma d(t)d^T(t)\Gamma] = D_{xx}\delta(t - \tau) \tag{9.6}$$

$$E[n(t)n^T(t)] = N_{uu}\delta(t - \tau) \tag{9.7}$$

where

$$D_{xx} = \begin{bmatrix} 0.0 & 0.0 & 0.0 \\ 0.0 & 100.0 & 0.0 \\ 0.0 & 0.0 & 1.0 \end{bmatrix}$$

and

$$N_{uu} = 1.0.$$

Using a control system design package MATRIX_x, the regulator and filter gain are respectively computed as

$$K = 1.0\text{E} + 05 \times [-0.0223 \quad 3.145 \quad -0.1024]$$

and

$$F = \begin{bmatrix} 0.1962 \\ 9.9998 \\ -0.0083 \end{bmatrix}$$

The frequency response of the open-loop transfer function of the closed-loop compensated system

$$\frac{y(s)}{r(s)} = \frac{\text{TANK LEVEL}}{\text{REFERENCE INPUT}} \tag{9.8}$$

where $y(s)$ is the tank level and $r(s)$ is the reference input, is shown in Fig. 9.4.

9.3 LQG/LTR CONTROLLER DESIGN

Now a tracking LQG/LTR controller design will be presented. This LQG/LTR control system has the structure shown in Fig. 9.3. This

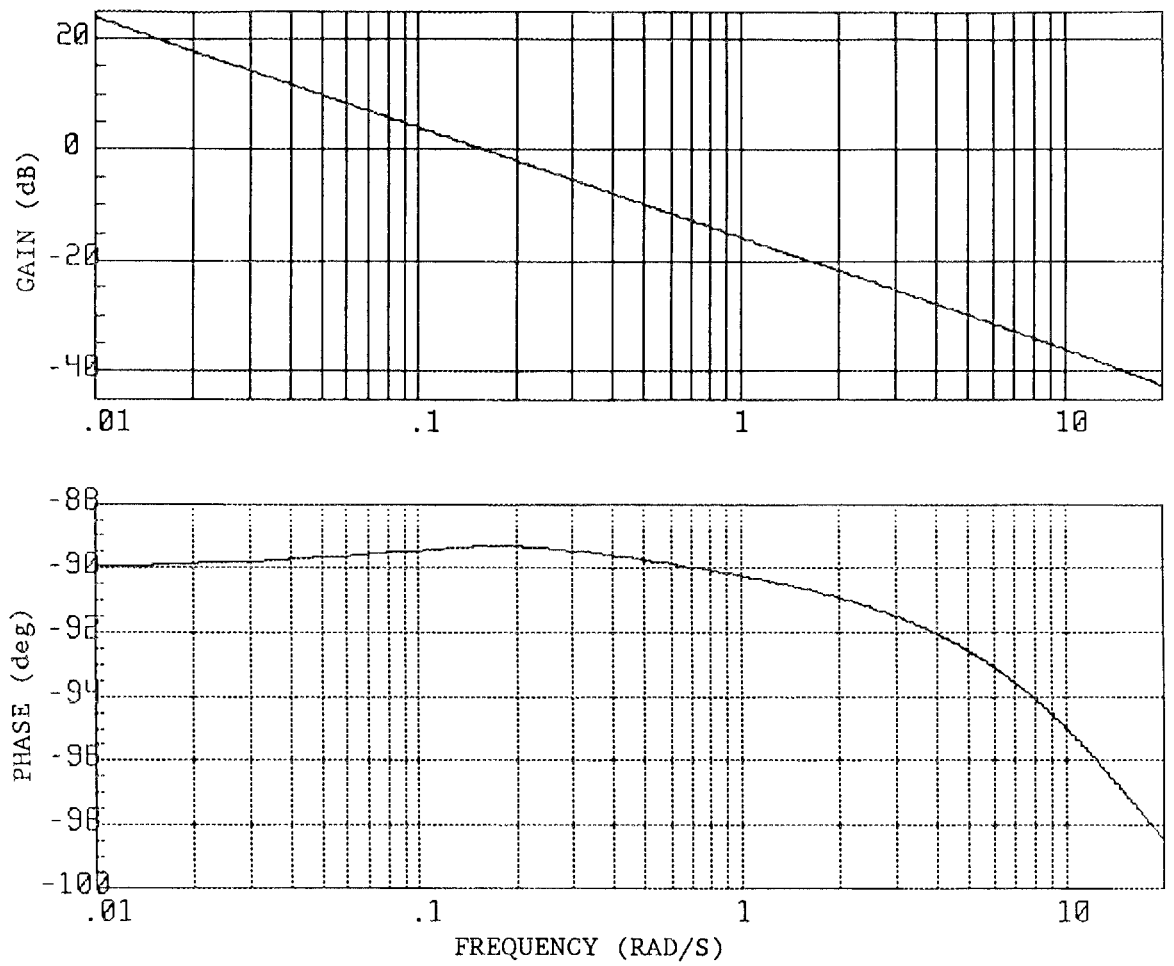

Fig. 9.4. Open-loop frequency response of the LQG control system.

LQG/LTR control system design is a two-step process. First, a Kalman filter (KBF) is designed to obtain good command following and disturbance rejection over a specified low-frequency range. Also, the KBF design is made to meet the required robustness criteria with system uncertainty of $\Delta L(s)$ at the system's output. It will be required to obtain good command following and disturbance rejection that

$$\sigma_{\min}(L_4(s)) \geq 20\ dB \qquad \forall\omega < 0.1 \text{ rad/s} \tag{9.9}$$

where $L_4(s)$ is the loop transfer function at the output of the KBF (point 4 of Fig. 9.2). Assuming the high-frequency uncertainty $\Delta L(s)$ for this system becomes significant at 5 rad/s, then for robustness it will be required that

$$\sigma_{\min}\{I + [L_4(s)]^{-1}\} \geq \|\Delta L(jw)\| = 5 \text{ dB} \qquad \forall\omega \geq 5 \text{ rad/s} \quad . \tag{9.10}$$

In this application the frequency at which system uncertainty becomes significant, 5 rad/s, and the magnitude of the uncertainty, 5dB at

5 rad/s, are assumed values. This assumption is required because of the lack of information on the model of the high-frequency modelling errors of the process being studied.

The second step is to recover the good robustness properties of the loop transfer function $L_4(s)$ of point 4 at the output node y (point 3). This will be accomplished by applying the loop transfer recovery (LTR) step at the output node (point 3). The LTR step requires the computation of a regulator gain (K) to obtain the robustness properties of the loop transfer function $L_4(s)$ at the output node y.

A tool exists that is used to obtain the LQG/LTR design for this system, considering the low- and high-frequency bound requirements. The tool used is CASCADE, a computer-aided system and control analysis and design environment that synthesizes the LQG/LTR design procedure.

The weighting matrices used in the design of the KBF are

$$D_{xx} = \begin{bmatrix} 3.775\text{E-}23 & 3.414\text{E-}18 & -1.272\text{E-}19 \\ 3.414\text{E-}18 & 3.088\text{E-}13 & -1.150\text{E-}14 \\ -1.272\text{E-}19 & -1.150\text{E-}14 & 4.284\text{E-}16 \end{bmatrix}$$

and

$$N_{uu} = \mu I = 0.25 \times 10^{-10} \quad .$$

The weighting matrices used in the LQR design of the loop transfer recovery (LTR) step are

$$Q = Q_o + q^2 C^T C = 10^6 \times \begin{bmatrix} 0.0 & 0.0 & 0.0 \\ 0.0 & 5.3866 & 0.1049 \\ 0.0 & 0.1049 & 0.002 \end{bmatrix}$$

where

$$Q_o = \begin{bmatrix} 1.0 & 0.0 & 0.0 \\ 0.0 & 100.0 & 0.0 \\ 0.0 & 0.0 & 1.0 \end{bmatrix}$$

and

$$R = 1.0 \quad .$$

The resulting filter and regulator gains for this system are respectively

$$F = \begin{bmatrix} 1.07\text{E-}02 \\ 0.472 \\ -2.299\text{E-}02 \end{bmatrix}$$

and

$$K = [0.660 \quad 27703.397 \quad 589.452] \quad .$$

The resulting open-loop frequency response of the compensated system is shown in Fig. 9.5.

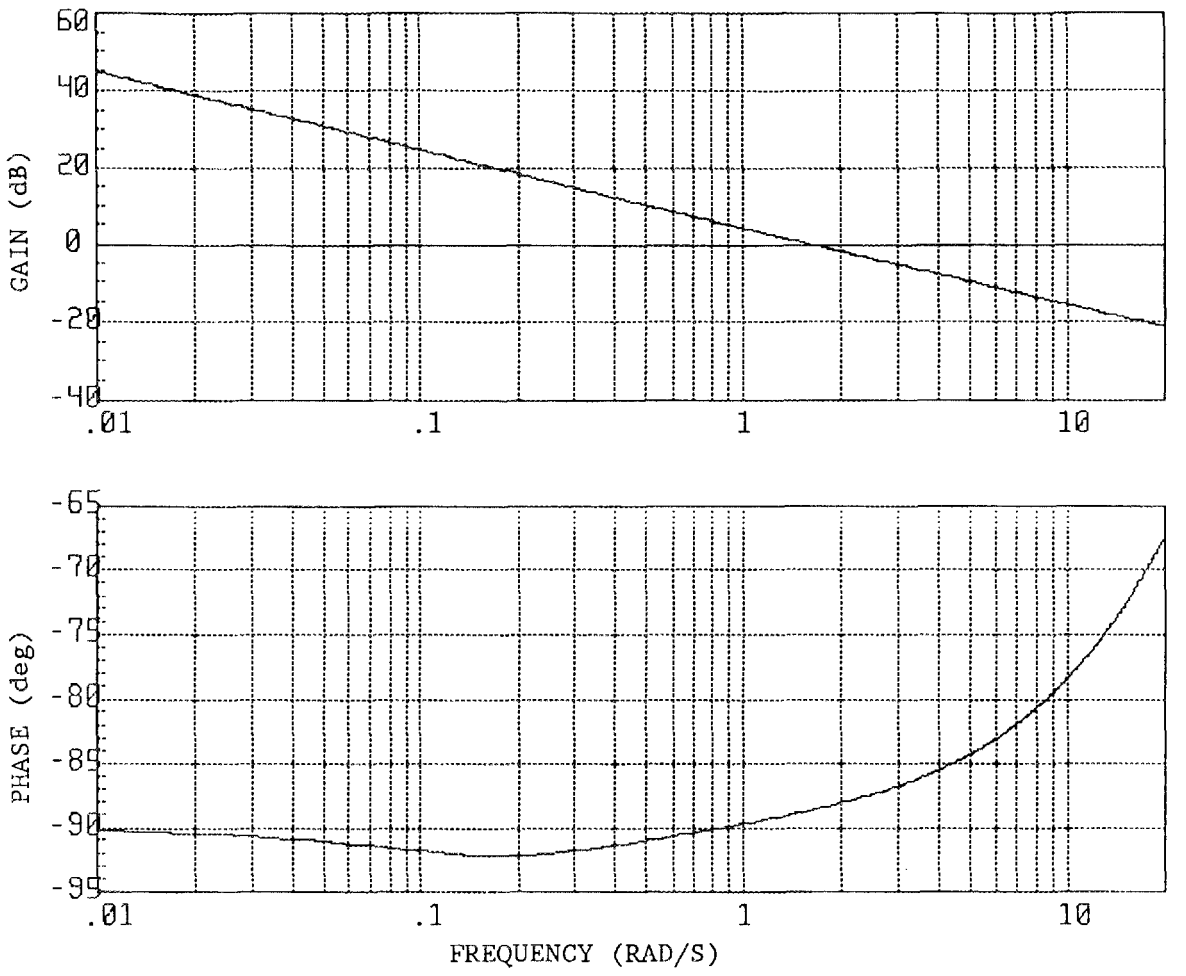

Fig. 9.5. Open-loop frequency response of the LQG/LTR control system.

9.4 PI CONTROLLER DESIGN

Now the design requirements for the PI control will be discussed. The PI controller for this system design will take on a structure similar to the three-element controller prevalent in process control. Therefore the PI control system structure will take the form shown in Fig. 9.6. (The classical design of the deaerator is discussed in Appendix B.)

The transfer functions used in this control structure are defined as

$$\frac{w(s)}{u(s)} = \frac{\text{CONDENSATE FLOW}}{\text{CONTROLLER OUTPUT}} \tag{9.11}$$

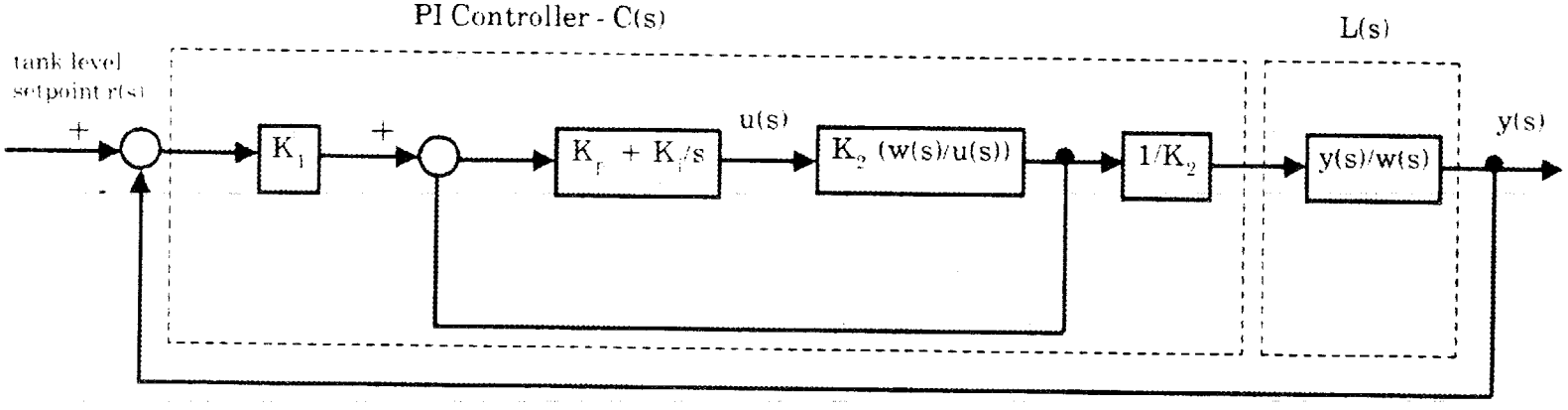

Fig. 9.6. Block diagram of PI control system.

and

$$\frac{y(s)}{w(s)} = \frac{\text{TANK LEVEL}}{\text{CONDENSATE FLOW}} \tag{9.12}$$

The constants K_1 and K_2 are used for unit conversion and defined respectively as 1.0 and 10^{-6}. The terms K_p and K_i are defined respectively as the proportional gain and the integral gain.

Using the practical experience of a prior three-element controller design, the proportional and integral gains are selected to be

$$K_p = 0.1$$

and

$$K_i = 0.05 \quad .$$

The resulting open-loop frequency response plot of the compensated system $y(s)/r(s)$ is shown in Fig. 9.7. The poles and transmission zeros of the original plant and the return ratios for the LQG, LQG/LTR, and PI control systems are shown in Tables 2, 3, and 4 respectively.

9.5 PRECOMPENSATOR DESIGN

The transient responses of the PI, LQG, and LQG/LTR control systems are shown respectively in Figs. 9.8, 9.9, and 9.10. The transient response of the LQG/LTR controller is seen to have a faster time to peak than the LQG and PI transient responses. Considering the practical physical limitations of the plant, it appears unlikely that the required rise time dictated by the transient response of the LQG/LTR is possible. It appears that the obvious solution would be to redesign the LQG/LTR control system to obtain a slower, more practical response. In the case of the LQG/LTR control system, the possibility of a redesign is eliminated, because the control system was designed to meet certain command tracking, disturbance rejection, and stability robustness requirements.

Therefore, to eliminate this difficulty, a second-order precompensator will be placed in the forward path of the reference input signal. This precompensator will shape the output transient response of the system, since the control system design requires the output to follow the reference input. The precompensator in this investigation will be required to have a time to peak of 30 s with a maximum overshoot of about 3%. The requirements are selected to somewhat emulate the transient response of the PI controller.

The transfer function of the second-order precompensator used is as follows:

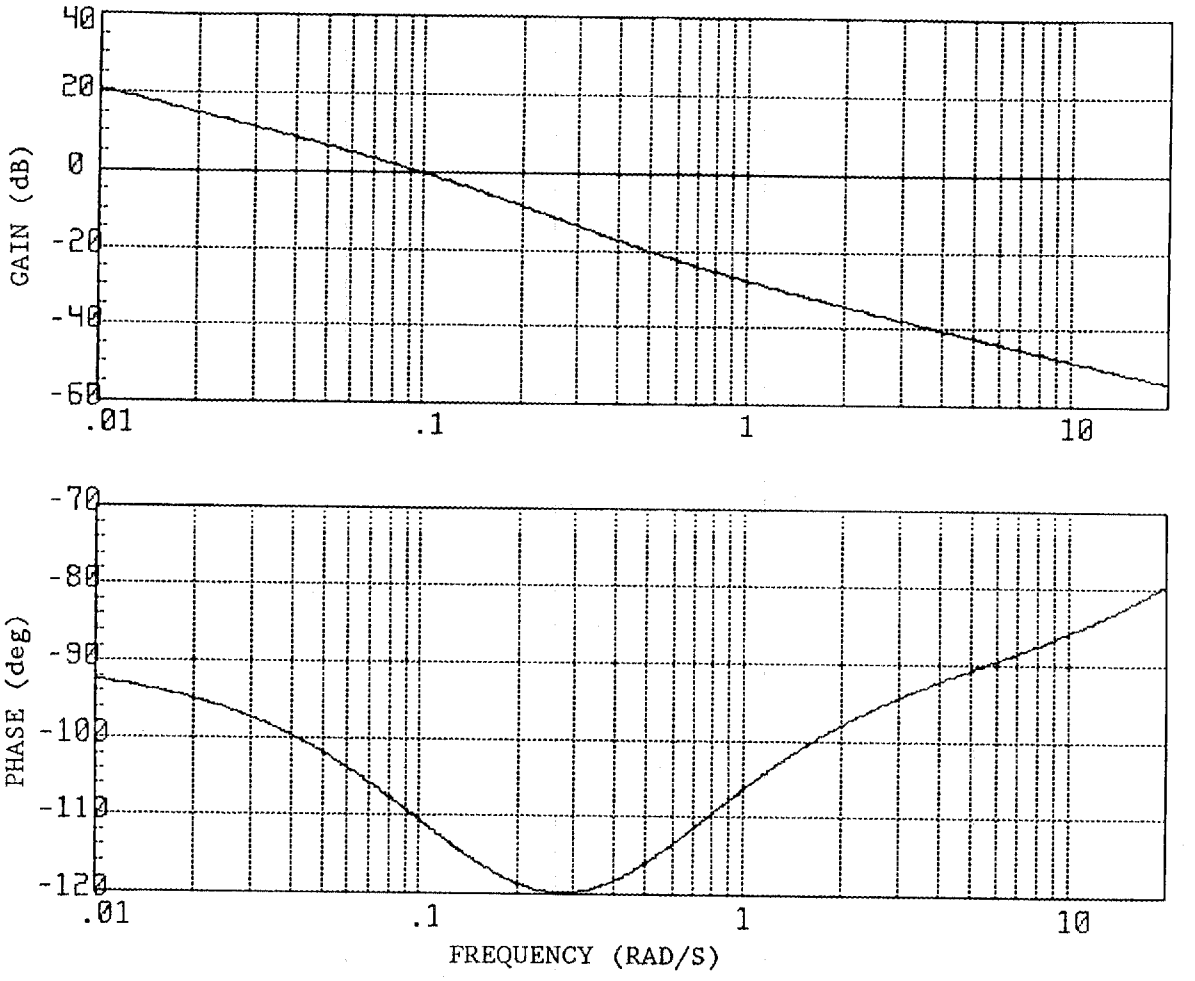

Fig. 9.7. Open-loop frequency response of PI control system.

Table 2. LQG controller and deaerator poles and zeros[a]

Poles		Zeros	
(1)	1.99E-06	(1)	−0.140
(2)	−0.141	(2)	−0.199
(3)	−0.204	(3)	−47.5
(4)	−32.9	(4)	−53.8
(5)	−53.8		

[a]Note: System gain = 2.3899E + 06.

Table 3. LQG/LTR controller and deaerator poles and zeros[a]

Poles		Zeros	
(1)	1.99E-06	(1)	−0.140
(2)	−0.141	(2)	−0.199
(3)	−0.181	(3)	−47.5
(4)	−47.7+j537.3		
(5)	−47.7−j537.3		
(6)	−53.8		

[a]Note: System gain = 9.9190E + 03.

Table 4. PI controller and deaerator poles and zeros[a]

Poles		Zeros	
(1)	0	(1)	−0.5
(2)	−0.143	(2)	−0.199
(3)	−0.227	(3)	−47.5
(4)	−98.8		

[a]Note: System gain = 0.076.

$$\frac{r(s)}{r_{in}(s)} = \frac{\omega_n^2}{s^2 + 2\zeta\omega_n s + \omega_n^2} \tag{9.13}$$

where ζ is the damping ratio, ω_n is the natural frequency, $r(s)$ is the output of the precompensator, and $r_{in}(s)$ is the actual reference input. The precompensator Eq. (9.13) can be represented in state equation form as follows:

$$\begin{bmatrix} \dot{x}_1 \\ \dot{x}_2 \end{bmatrix} = \begin{bmatrix} 0 & 1 \\ -\omega_n^2 & -2\zeta\omega_n \end{bmatrix} \begin{bmatrix} x_1 \\ x_2 \end{bmatrix} + \begin{bmatrix} 0 \\ 1 \end{bmatrix} r_{in}(t) \tag{9.14}$$

and

$$r(t) = [\ \omega_n^2 \quad 0] \begin{bmatrix} x_1 \\ x_2 \end{bmatrix} \tag{9.15}$$

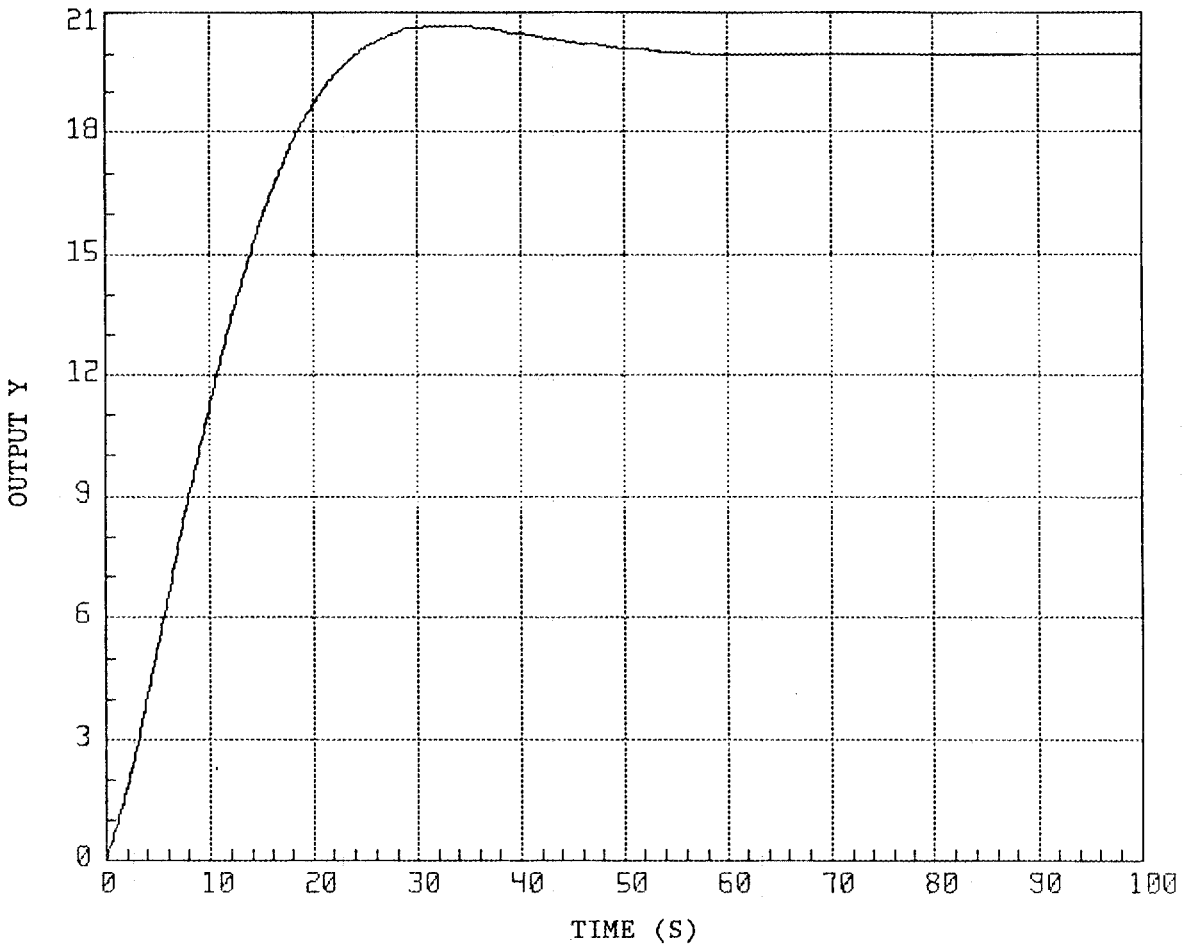

Fig. 9.8. PI control system closed-loop transient response.

where $r_{in}(t)$ is the time domain representation of the reference input signal and $r(t)$ is the time domain signal at the output of the precompensator.

Considering the 3% overshoot requirement, then ζ must be 0.7. Using the following expression,

$$t_{max} = \frac{\pi}{\omega_n\sqrt{1 - \zeta^2}} \tag{9.16}$$

where t_{max} must be 30 s, then

$$\omega_n = \frac{\pi}{30\sqrt{1 - (.7)^2}} \quad . \tag{9.17}$$

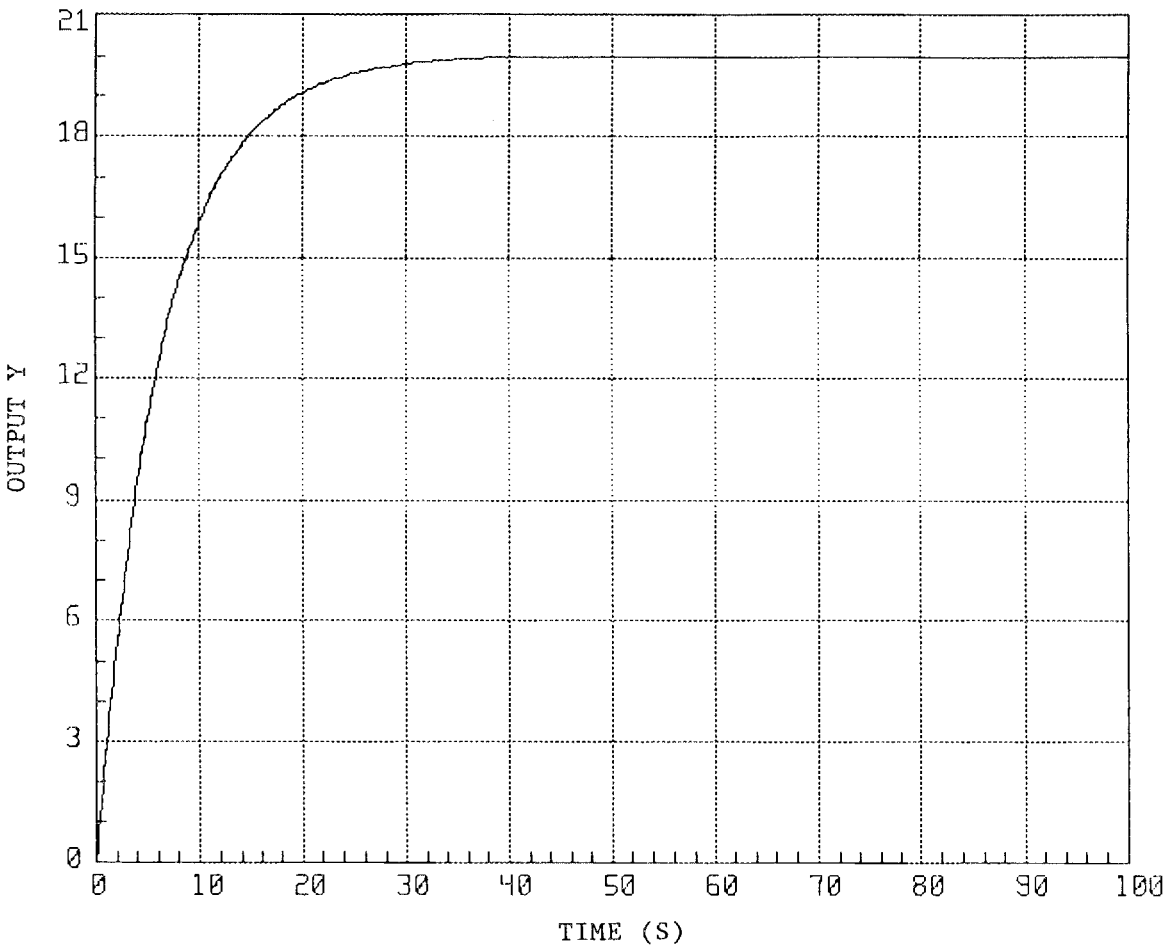

Fig. 9.9. LQG control system closed-loop transient response.

Now the complete state equation of the precompensator is given as

$$\begin{bmatrix} \dot{x}_1 \\ \dot{x}_2 \end{bmatrix} = \begin{bmatrix} 0 & 1 \\ -0.0215 & -0.2052 \end{bmatrix} \begin{bmatrix} x_1 \\ x_2 \end{bmatrix} + \begin{bmatrix} 0 \\ 1 \end{bmatrix} r_{in}(t) \qquad (9.18)$$

and

$$r(t) = [0.0215 \quad 0] \begin{bmatrix} x_1 \\ x_2 \end{bmatrix} . \qquad (9.19)$$

The resulting transient response of the LQG/LTR control system using the precompensator is shown in Fig. 9.11.

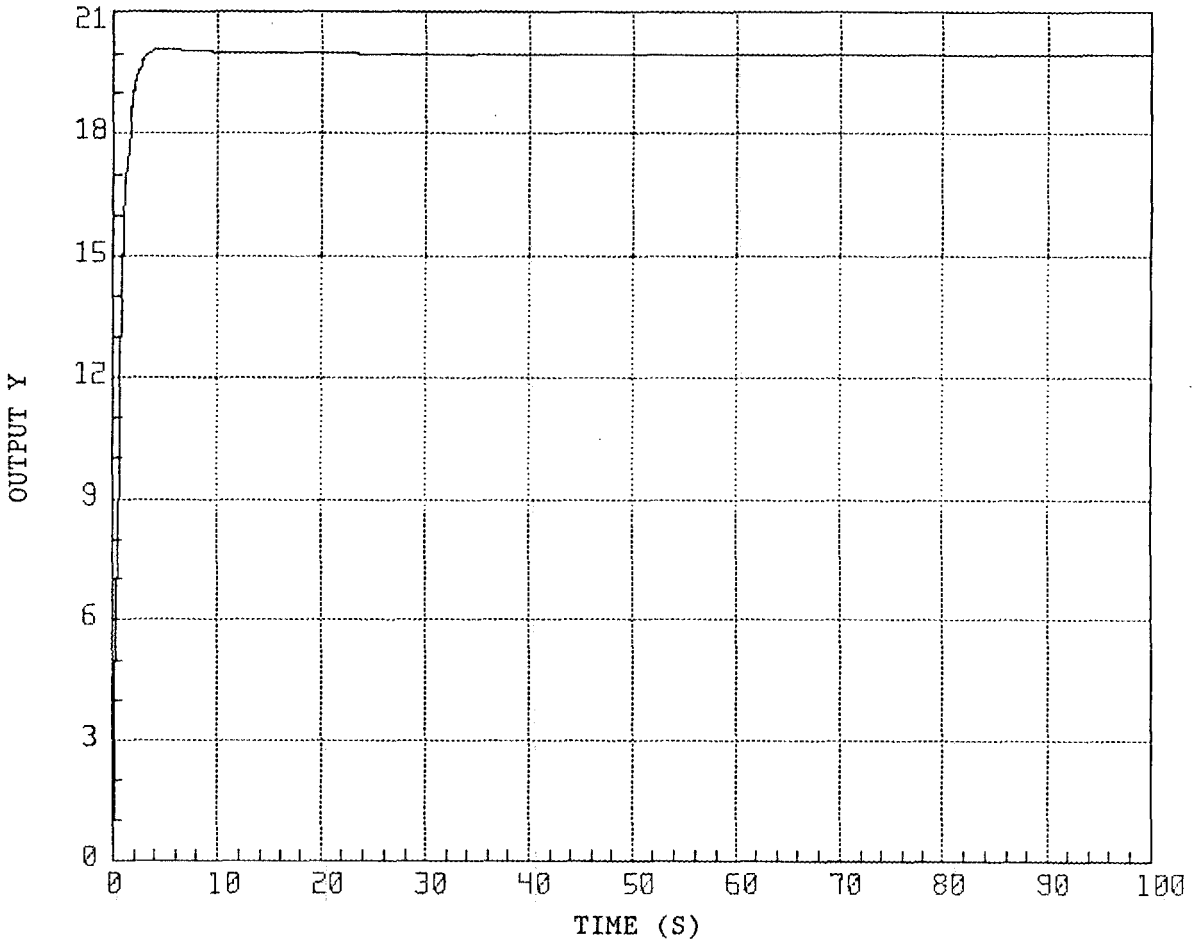

Fig. 9.10. LQG/LTR control system closed-loop transient response.

9.6 ANALYSIS OF SINGULAR-VALUE PLOTS

Using the singular-value plots of the return ratio, inverse return difference, and return difference, the performance and stability robustness characteristics of the various deaerator control system designs can be examined. Recall that systems with large stability margins, good disturbance rejection/command following, low sensitivity to plant parameter variations, and stability in the presence of model uncertainties are described as being robust and having good robustness properties. The singular-value plots for the PI, LQG, and LQG/LTR control systems will therefore be examined to evaluate the robustness properties of each system. An explanation of the relationship between the singular-value plots and the performance robustness properties is given in Appendix A.

9.6.1 PI Control System Singular-Value Plots

First let us define for the singular-value plots the return ratio $L(s)$, which contains the transfer function of both the compensator and the

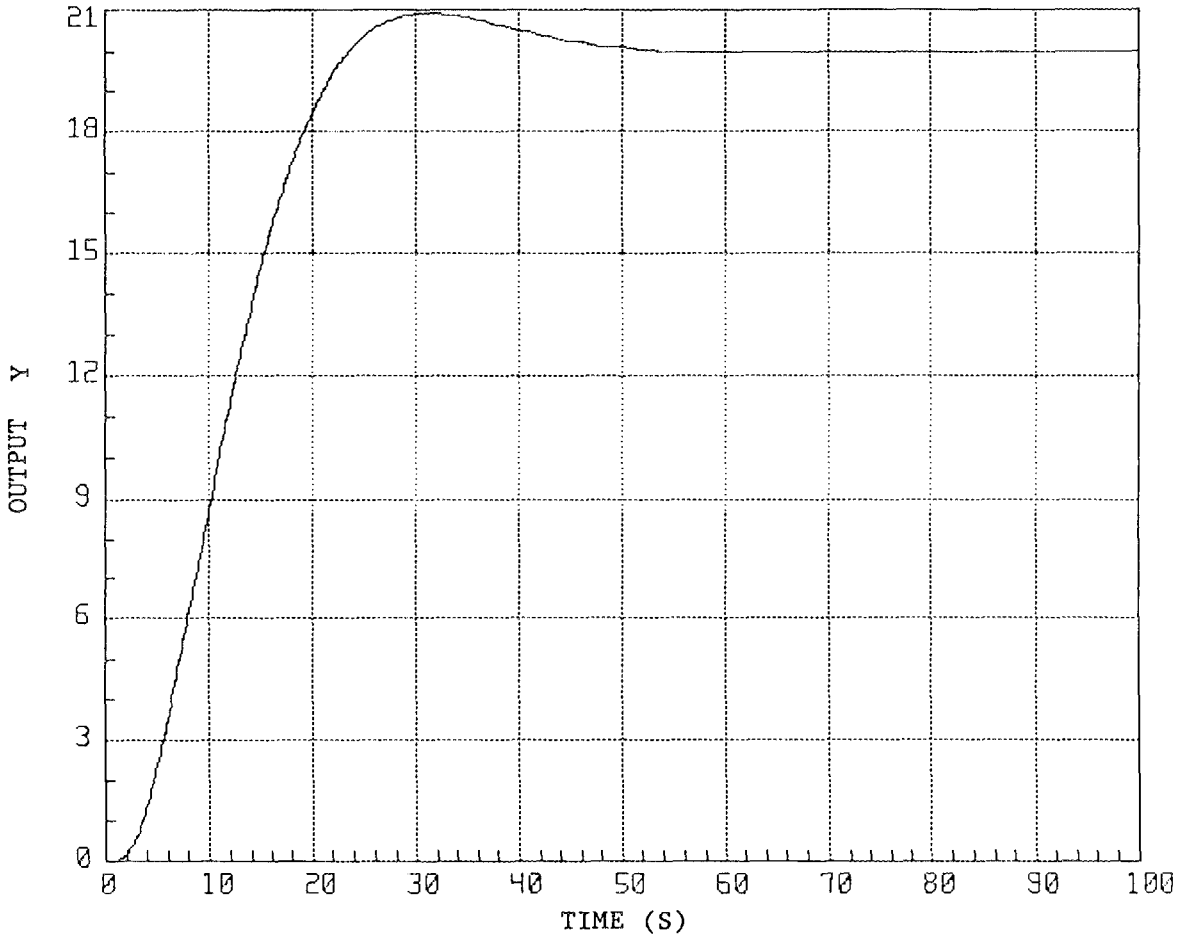

Fig. 9.11. LQG/LTR control system design closed-loop transient response with precompensator.

plant for a given control system. The PI control system return ratio singular-value plot (RSV) shown in Fig. 9.12 indicates that at low frequencies the system has good disturbance-rejection properties for $\sigma_{\min}(L(j\omega)) \geq 20$ dB at $\omega \leq 0.01$ rad/s. The command-following property of the PI controller yields a steady state error of zero. The good command-following property for a step reference input exists for the PI controller because the plant is a type 1. The PI controller does very well at minimizing the effect of sensor noise as a result of the very small gain at high frequencies. The approximate crossover frequency for this system is 0.1 rad/s, as observed from the RSV.

To minimize sensitivity of the closed-loop system to parameter variations, the return difference singular-value plot (RDSV), as discussed previously, requires that

$$\sigma_{\min}[I + L(j\omega)] >> 1 \quad \forall\ \omega \epsilon\ F \tag{9.20}$$

where F is a low-frequency range where parameter variations occur. For a more specific analysis let us require

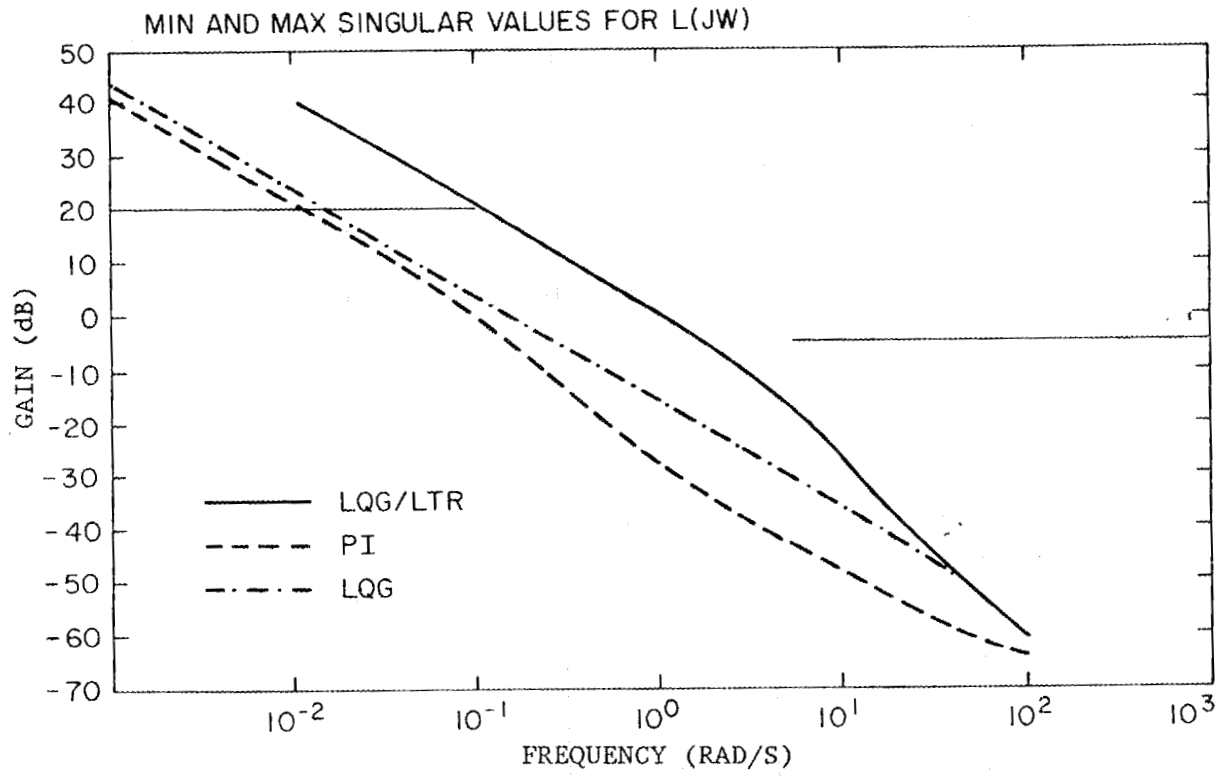

Fig. 9.12. Singular-value plots of return ratio.

$$\sigma_{\min}(I + L(j\omega)) \geq 20 \gg 1 \tag{9.21}$$

or

$$\sigma_{\min}(I + L(j\omega)) \geq 26 \text{ dB} \gg 0\text{dB} \tag{9.22}$$

over some range of ω.

Now considering the criteria of Eq. (9.22) and examining Fig. 9.13, the RDSV for the PI control system indicates that the PI control system output is insensitive to low-frequency parameter variations for $\omega \leq$ 0.0055 rad/s.

Next let us examine the inverse return difference singular-value plot (IRDSV) shown in Fig. 9.14 for the PI control system. The IRDSV indicates that the PI control system is stable in the presence of a high-frequency modelling error greater than the magnitude specified in Sect. 9.3.

9.6.2 LQG Control System Singular-Value Plots

The return ratio singular-value plot (RSV) for the LQG control system indicates that at low frequencies the system has good disturbance rejection properties for

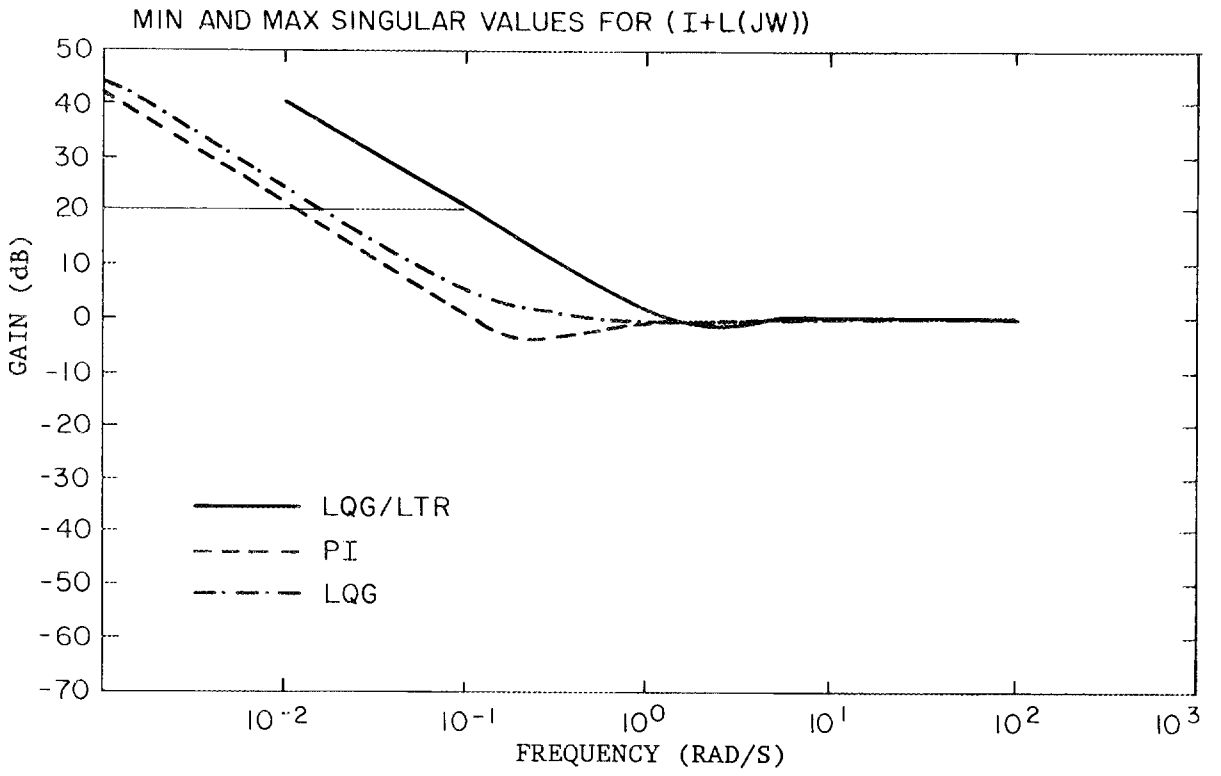

Fig. 9.13. Singular-value plots of return difference.

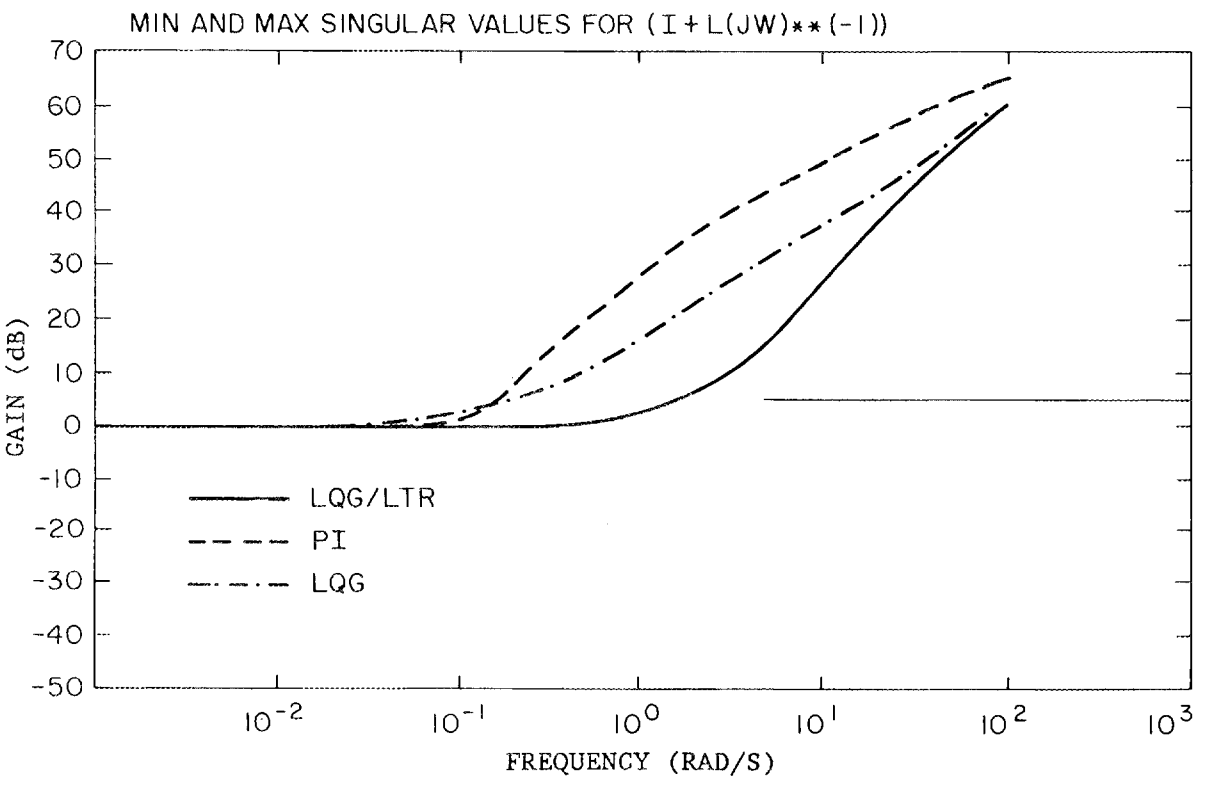

Fig. 9.14. Singular-value plots of inverse return difference.

$$\sigma_{\min}[L(j\omega)] \geq 20 \text{ dB}$$

where, in this case, $\omega \leq .017$ rad/s.

The RSV also reveals that the control system has good immunity to sensor noise, because of the significant attenuation of $L(j\omega)$ occurring at frequencies much greater than 1 rad/s. This attenuation also implies that good robustness properties can be expected when the inverse return difference is examined for stability to multiplicative plant perturbations.

The command-following property for this system is good for a step input, since the plant is a type 1 system. This good command-following property is also applicable to the LQG/LTR control system.

The sensitivity of the LQG control system is now examined using the criteria given in Eq. (9.21) The LQG control system satisfies the required conditions for $\omega \leq 0.008$ rad/s. Thus only for slowly varying parameters is the LQG control system output insensitive.

The IRSV of this control system implies that the system is certainly stable for a multiplicative plant perturbation such that

$$\|\Delta L(jw)\| = 5 \text{ dB} \quad \forall\ \omega \geq 5 \text{ rad/s}$$

since

$$\sigma_{\min}\{I + [L(jw)]^{-1}\} > 5 \text{ dB} \quad \forall\ \omega \geq 5 \text{ rad/s} \quad .$$

9.6.3 LQG/LTR Control System Singular-Value Plots

The LQG/LTR RSV indicates that the control system meets the requirements given in Eq. (9.9), thus ensuring a good disturbance-rejection property. The system output completely tracks the reference input, since the plant is a type 1 system. The approximate system crossover frequency is 1 rad/s according to the RSV. The RSV also indicates that the effects of sensor noise are significantly minimized at $\omega \geq 5$ rad/s.

The RDSV satisifies inequality (9.22) for $\omega \leq 0.055$ rad/s, thus ensuring a system insensitive to parameter variations only at low frequencies.

The IRSV shows that the LQG/LTR control system is very stable for the multiplicative perturbation ΔL specified in Sect. 9.3.

9.7 DEAERATOR STUDY SUMMARY AND CONCLUSIONS

9.7.1 Summary of Control System Analysis

The design criteria used for analysis in this system is defined as shown in Table 5. The performance and robustness results summarized from the analysis using the singular-value plots are shown in Table 6. From this

Table 5. System design specifications

System requirements	Range
Good command-following/disturbance rejection	$\sigma_{min}[L(j\omega)] > 20$ dB $\forall\omega \leq 0.1$ rad/s
Good system response to high-frequency modeling error	$\sigma_{min}\{I + [L(j\omega)]^{-1}\} \geq \|\Delta L\| = 5$ dB $\forall\omega \leq 5$ rad/s
Good insensitivity to parameter variations at low frequencies	$\sigma_{min}[I + L(j\omega)] \geq 26$ dB for low frequencies
Good immunity to noise $\omega \geq 5$ rad/s	$\sigma_{max}[L(j\omega)] \ll 0$ dB for high frequencies

table it appears that the LQG/LTR control system has the widest low-frequency range of disturbance rejection and insensitivity to parameter variations. The PI control system is seem to have the worst disturbance rejection property and the most sensitivity to parameter variations.

All of the control systems demonstrate the capability of maintaining a stable robust system in the presence of high-frequency modelling errors, especially the PI control system. Even though all the control systems also have good immunity to noise at frequencies significantly greater than 5 rad/s, the PI control system has the best immunity.

The LQG/LTR control system is seen to meet all the design criteria, unlike the other control systems. The design of the LQG/LTR control system was obtainable in a systematic manner, in contrast to the trial-and-error method used for the LQG control system. The LQG controller design was obtained by shaping of the output transient response using the system state weighting matrix, then examining the system's singular-value plots. The PI control system used is simply a three-element control system strategy that has previously been used in the simulation study of the deaerator flow control system.

9.7.2 Conclusions

It should be evident that performance characteristics such as a suitable transient response do not imply that the system will have good robustness properties. Obtaining suitable performance characteristics and a stable robust system are two completely separate goals. Presently and in the past, classical unity-feedback design methods have been used for transient response shaping, with little consideration for robustness

Table 6. Performance and robustness results

System properties	PI control system	LQG control system	LQG/LTR control system
Command following/ disturbance	$\sigma_{min}[L(j\omega)] \geq 20$ dB $\forall\ \omega \leq 0.01$ rad/s	$\sigma_{min}[L(j\omega)] \geq 20$ dB $\forall\ \omega \leq .017$ rad/s	$\sigma_{min}[L(j\omega)] \geq 20$ dB $\forall\ \omega \leq 0.1$ rad/s
System response to high frequency modeling error ($\omega \geq 5$ rad/s)	$\sigma_{min}\{I + [L(j\omega)]^{-1}\} \geq 43.0$ dB	$\sigma_{min}\{I + [L(j\omega)]^{-1}\} \geq 30$ dB	$\sigma_{min}\{I + [L(j\omega)]^{-1}\} \geq 16.7$ dB
Insensitivity to parameter variations at low frequencies	$\sigma_{min}[I + L(j\omega)] \geq 26$ dB $\forall\ \omega \leq 0.0055$ rad/s	$\sigma_{min}[I + L(j\omega)] \geq 26$ dB $\forall\ \omega \leq 0.008$ rad/s	$\sigma_{min}[I + L(j\omega)] \geq 26$ dB $\forall\ \omega \leq 0.055$ rad/s
Immunity to noise ($\omega \geq 5$ rad/s)	$\sigma_{max}[L(j\omega)] \leq -42.5$ dB	$\sigma_{max}[L(j\omega)] \leq -30$ dB	$\sigma_{max}[L(j\omega)] \leq -16$ dB

properties. The main advantage of having a closed-loop feedback system is that good performance and stability robustness properties are obtainable. As seen in this paper, transient response shaping can be obtained easily using a precompensator. Therefore it appears that the goal of the control system designer is first to design a stable robust system and then use prefiltering to obtain the desired transient response.

Optimal control methods as demonstrated by the LQG control system do not guarantee good robustness properties when applied systematically to meet minimization requirements of a performance index. Methods such as pole placement emphasize transient response characteristic without regard to robustness, which could be detrimental to the system integrity in the presence of model uncertainties.

REFERENCES

1. M. G. Safonov, A. J. Laub, and G. L. Hartmann, "Feedback Properties of Multivariable Systems: The Role and Use of the Return Difference Matrix," IEEE Trans. Autom. Control, **AC-26**, 47-65 (February 1981).

2. M. G. Safonov and M. Athans, "Gain and Phase Margin for Multiloop LQG Regulators," IEEE Trans. Autom. Control, **AC-22**, 173-179 (April 1977).

3. G. Stein and M. Athans, "The LQG/LTR Procedure for Multivariable Feedback Control Design," IEEE Trans. Autom. Control, **AC-32**, 105-114 (February 1987).

4. J. D. Birdwell, J. R. B. Cockett, R. E. Bodenheimer, and G. Chang, The CASCADE Final Report: Volume II--CASCADE Tools and Knowledge Base, Electrical Engineering Department, The University of Tennessee, Knoxville, Feb. 19, 1988.

5. H. Kwakernaak and R. Sivan, Linear Optimal Control Systems, Wiley-Interscience, New York, 1972.

6. J. D. Birdwell, class notes of Modern Control Theory, EE 5291, Electrical Engineering Department, The University of Tennessee, Knoxville, Spring 1986.

7. J. B. Cruz, Jr., and W. R. Perkins, "A New Approach to the Sensitivity Problem in Multivariable Feedback System Design," IEEE Trans. Autom. Control, **AC-9**, 216-223 (July 1964).

APPENDIX A

Appendix A

SINGULAR-VALUE REQUIREMENTS FOR SYSTEM DESIGN

First let us derive the representation of $y(s)$. From Fig. A1, it can be shown that

$$y(s) = [L(s)K(s)]e(s) + d(s) \tag{A1}$$

where

$$e(s) = r(s) - y(s) - n(s) \tag{A2}$$

thus

$$y(s) = [L(s)K(s)][r(s) - y(s) - n(s)] + d(s) \tag{A3}$$

$$y(s) = L(s)K(s)r(s) - L(s)K(s)y(s) - L(s)K(s)n(s) + d(s)$$

therefore

$$\begin{aligned} y(s) &= [I + L(s)K(s)]^{-1}[L(s)K(s)r(s) - L(s)K(s)n(s) + d(s)] \\ &= [I + L(s)K(s)]^{-1}[L(s)K(s)[r(s) - n(s)]] \\ &\quad + [I + L(s)K(s)]^{-1}d(s) \\ &= y_r(s) + y_d(s) - y_n(s) \end{aligned} \tag{A4}$$

where $y_r(s)$, $y_d(s)$ and $y_n(s)$ are respectively the contributions to the plant output due to the reference input, disturbance input, and noise input to the system. Now the requirements for good command following, disturbance rejection, and insensitivity to sensor noise will be defined using singular values to characterize the magnitude of MIMO transfer functions. These requirements are also applicable to SISO systems.[1]

Singular-Value Requirements for Good Command Following

Good command following of the reference input $r(t)$ by the plant output $y(t)$ implies that

$$y(s) \approx r(s) \qquad \forall s \epsilon s_R \tag{A5}$$

where s_R is the imaginary frequency range of the input $r(s)$. Letting $d(s) = n(s) = 0$ in Eq. (A4) results in

$$y_R(s) = [I + L(s)K(s)]^{-1}L(s)K(s)r(s) \quad . \tag{A6}$$

Therefore, to obtain good command following for this system requires that

$$\sigma_{min}(L(j\omega)K(j\omega)) >> 1 \qquad \forall \omega \epsilon \omega_R \quad . \tag{A7}$$

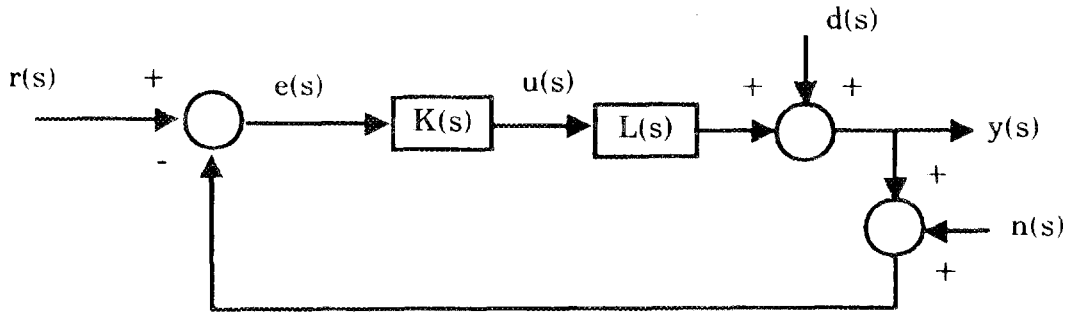

$r(s)$	- input reference signal
$e(s)$	- error signal transfer function
$u(s)$	- input signal to plant transfer function
$d(s)$	- disturbance signal transfer function
$y(s)$	- output signal transfer function
$n(s)$	- noise signal transfer function
$L(s)$	- nominal plant transfer function
$K(s)$	- compensator transfer function
ω_R	- frequency range of the input command
ω_d	- frequency range of the distance
ω_N	- frequency range of the noise
s	- imaginary frequency $j\omega$

Fig. A1. Unity feedback MIMO control system.

Singular-Value Requirements for Good Disturbance Rejection

To minimize the effect of disturbance on the output signal $y(s)$, Eq. (A4) will be examined when $n(s) = r(s) = 0$, which results in

$$y_d(s) = [I + L(s)K(s)]^{-1}d(s) \quad . \tag{A8}$$

Good disturbance rejection at the plant output requires

$$\sigma_{min}(L(j\omega)K(j\omega)) >> 1 \qquad \forall\omega\epsilon\omega_d \quad . \tag{A9}$$

Singular-Value Requirements for Good Immunity to Sensor Noise

First letting $r(s) = d(s) = 0$ in Eq. (A4) results in

$$y_n(s) = -[I + L(s)K(s)]^{-1}(L(s)K(s)n(s)) \quad . \tag{A10}$$

Therefore to minimize $y_n(s)$ requires that

$$\sigma_{max}(L(j\omega)K(j\omega)) << 1 \qquad \forall\omega\epsilon\omega_n \quad . \tag{A11}$$

It is apparent that any overlapping of any of the frequency ranges ω_R, ω_d, or ω_n will require system design specification trade-offs to be made. This will definitely occur when overlapping of the lower frequency ranges of ω_R and/or ω_d with the higher frequency range ω_n occurs.

APPENDIX A REFERENCE

1. H. Kazerooni and K. Narayanan, "Loop Shaping Design Related to LQG/LTR for SISO Minimum Phase Plants," American Control Conference, 1, 512-519 (June 1987); IEEE, 1987.

APPENDIX B

Appendix B

CLASSICAL DESIGN OF THE DEAERATOR CONTROL SYSTEM

This procedure summarizes the design of the deaerator control system in which classical techniques (root loci and Bode plots) were utilized and will be used in comparison with the robust control system. A general model of the deaerator is shown in Fig. B1. The appropriate linearized transfer functions obtained from the modular modeling systems (MMS) developed by Babcock and Wilcox for the Electric Power Research Institute (EPRI) are

$$\frac{y(s)}{u(s)} = \frac{0.76\ (s^2 + 47.66s + 9.423)}{s^3 + 53.9423s^2 + 7.5587s - 1.5039 \times 10^{-5}} \tag{B1}$$

and

$$\frac{w(s)}{u(s)} = \frac{4.5227 \times 10^8 s^2 + 6.424 \times 10^7 s - 77.546}{s^3 + 53.9423s^2 + 7.5587s - 1.5039 \times 10^{-5}} \tag{B2}$$

where

$y(s)$ - deaerator tank level
$w(s)$ - condensate flow
$u(s)$ - control action of the valve

The first step in the design process is to factor the two transfer functions to emphasize their pole-zero locations. Thus

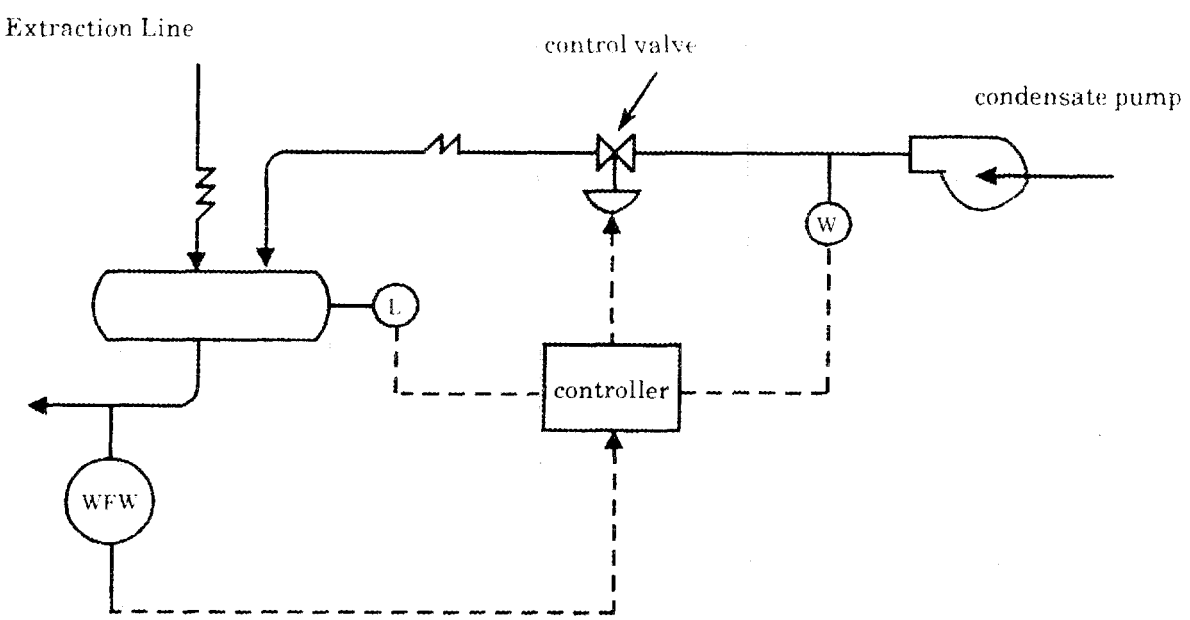

Fig. B1. General process flow diagram of the deaerator.

$$\frac{y(s)}{u(s)} = \frac{0.76(s + 0.1986)(s + 47.458)}{(s - 1.9896 \times 10^{-6})(s + 0.1405)(s + 53.8015)} \tag{B3}$$

and

$$\frac{w(s)}{u(s)} = \frac{4.5227 \times 10^{8}(s + 1.2071 \times 10^{-6})(s + 0.142)}{(s - 1.9896 \times 10^{-6})(s + 0.1405)(s + 53.8015)} \quad . \tag{B4}$$

At first glance it would seem that these two transfer functions, Eqs. (B3) and (B4), have right half plane poles and zeroes. However these poles and zeroes average due to numerical inaccuracies in the linearization process in the MMS digital simulation program. A more realistic set of transfer functions is

$$\frac{y(s)}{u(s)} = 0.76 \frac{(s + 0.1986)(s + 47.458)}{s(s + 0.1405)(s + 53.8015)} \tag{B5}$$

and

$$\frac{w(s)}{u(s)} = 4.5227 \times 10^{8} \frac{s + 0.142}{(s + 0.1405)(s + 53.8015)} \quad . \tag{B6}$$

To facilitate the design process, Eqs. (B5) and (B6) are further manipulated to obtain the two transfer functions

$$\frac{w(s)}{u(s)} = 4.5227 \times 10^{8} \frac{s + 0.142}{(s + 0.1405)(s + 53.8015)} \tag{B7}$$

and

$$\frac{y(s)}{w(s)} = 1.6804 \times 10^{-9} \frac{(s + 0.1986)(s + 47.458)}{s(s + 0.142)} \tag{B8}$$

With the transfer functions in this form, the block diagram of the system has an inner and an outer loop, as shown in Fig. B2.

The variable WFW represents the feedwater flow. However, for this study it was maintained constant. A PI controller was utilized in this application. The system shown in Fig. B2 can now be cast in the form of a system with unity feedback, as shown in Fig. B3.

In this formulation the poles and zeros of the closed inner loop appear in the open outer-loop transfer function. The procedure then starts with the open inner loop, whose transfer function $F_{IL}(s)$ is

$$F_{IL}(s) = K_p\left(s + \frac{k_i}{k_p}\right) \times K_3 \times 4.5227 \times 10^{8} \times \frac{(s + 0.142)}{s(s + 0.1405)(s + 53.801)} \tag{B9}$$

The root locus of the inner loop is sketched in Fig. B4. It is seen that there is a great deal of freedom in the choice of the zero in the controller transfer functions.

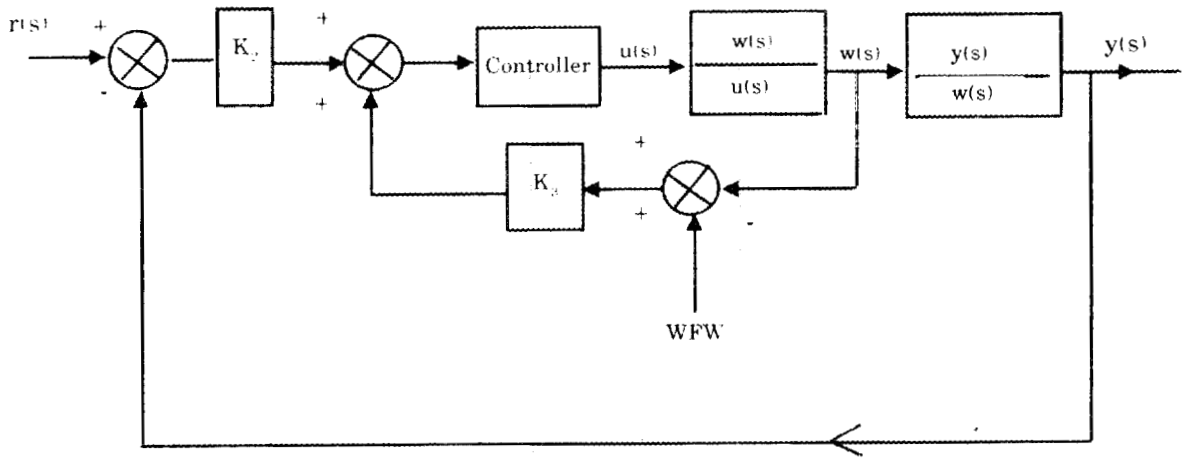

Fig. B2. Block diagram of the linearized system.

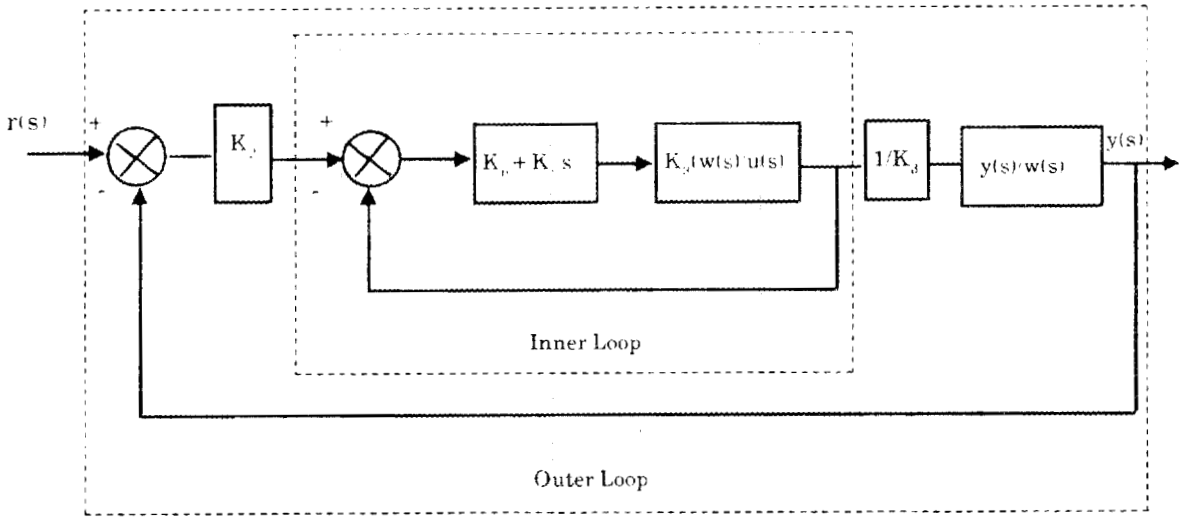

Fig. B3. Linearized system with unity feedback.

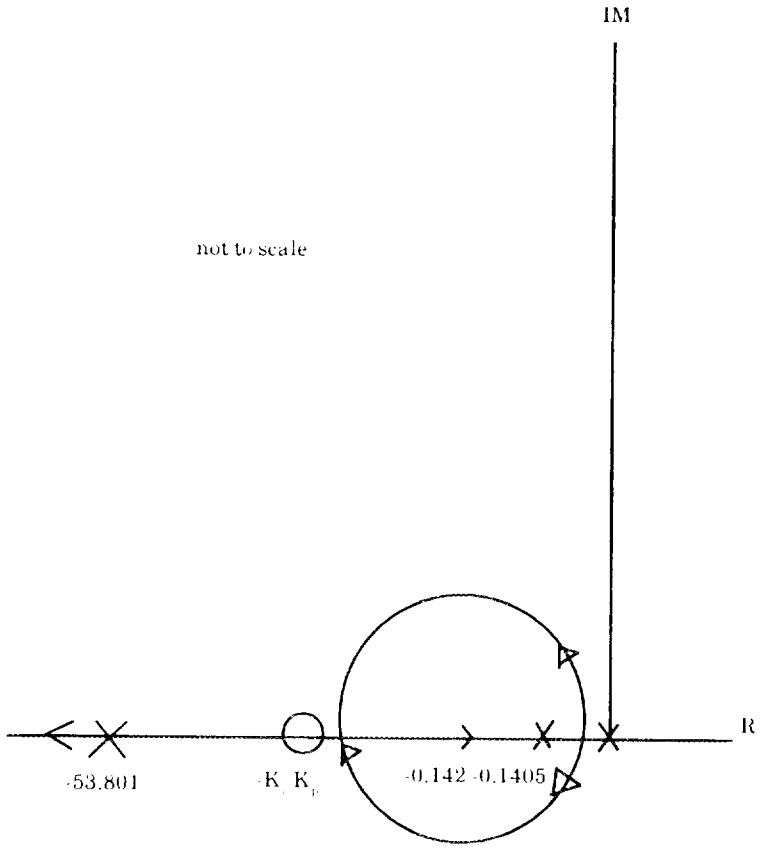

Fig. B4. Sketch of inner loop root locus.

Reasonable values are

$$K_p = 0.1$$

$$K_i = 0.05$$

and

$$K_3 = 1 \times 10^{-6} \quad .$$

The closed inner loop F_{ILC} now has the transfer function

$$F_{ILC}(s) = 45.227 \frac{(s + 0.142)(s + 0.5)}{(s + 98.8)(s + 0.1432)(s + 0.2268)} \quad . \qquad \text{(B10)}$$

The open outer loop $F_{OL}(s)$ now becomes

$$F_{OL}(s) = \frac{45.227 * 1.6804 \times 10^{-9}}{1 \times 10^{-6}}$$

$$\frac{(s + 0.5)(s + 0.142)(s + 0.1986)(s + 47.458)}{s(s + 98.8)(s + 0.1432)(s + 0.2268)(s + 0.142)} \tag{B11}$$

or

$$F_{OL}(s) = 0.076 \frac{(s + 0.5)(s + 0.1986)(s + 47.458)}{s(s + 98.8)(s + 0.1432)(s + 0.2268)} \tag{B12}$$

The closed outer loop F_{OLC} now becomes

$$F_{OLC}(s) = 0.076 \frac{(s + 0.5)(s + 0.1986)(s + 47.458)}{s(s + 98.84)(s + 0.2159)(s^2 + 0.1913s + 0.0168)} . \tag{B13}$$

A sketch of the open loop root locus $F_{OLC}(s)$ is shown in Fig. B5. The frequency of $F_{ILC}(s)$ and $F_{OLC}(s)$ are shown respectively in Figs. B6 and B7.

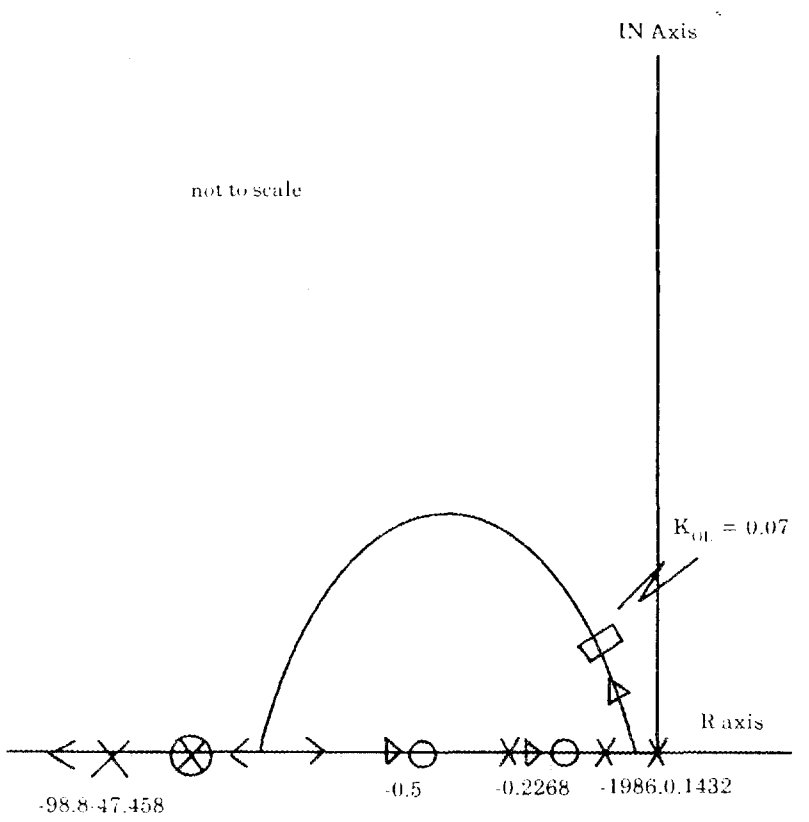

Fig. B5. Outer loop root locus.

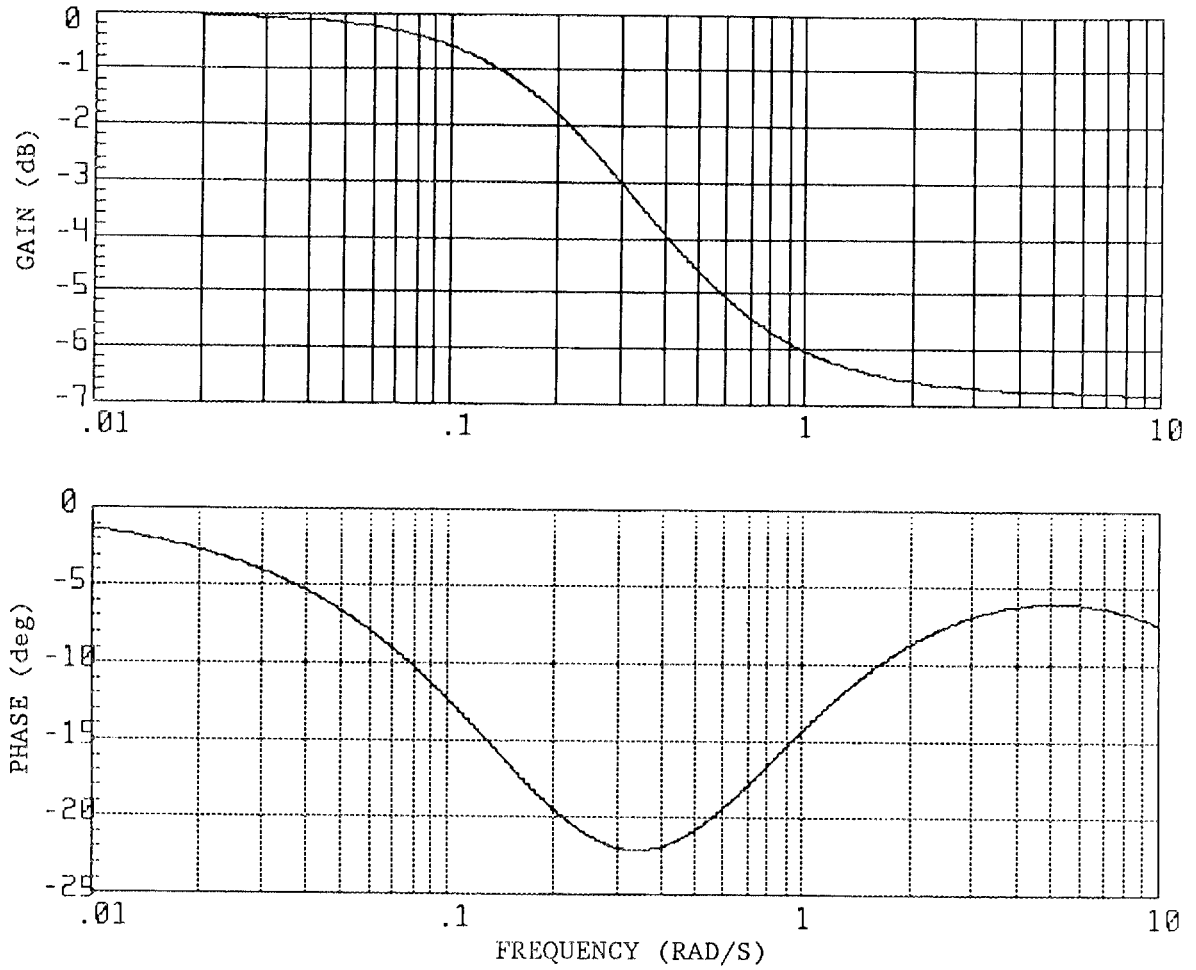

Fig. B6. Frequency response of inner loop.

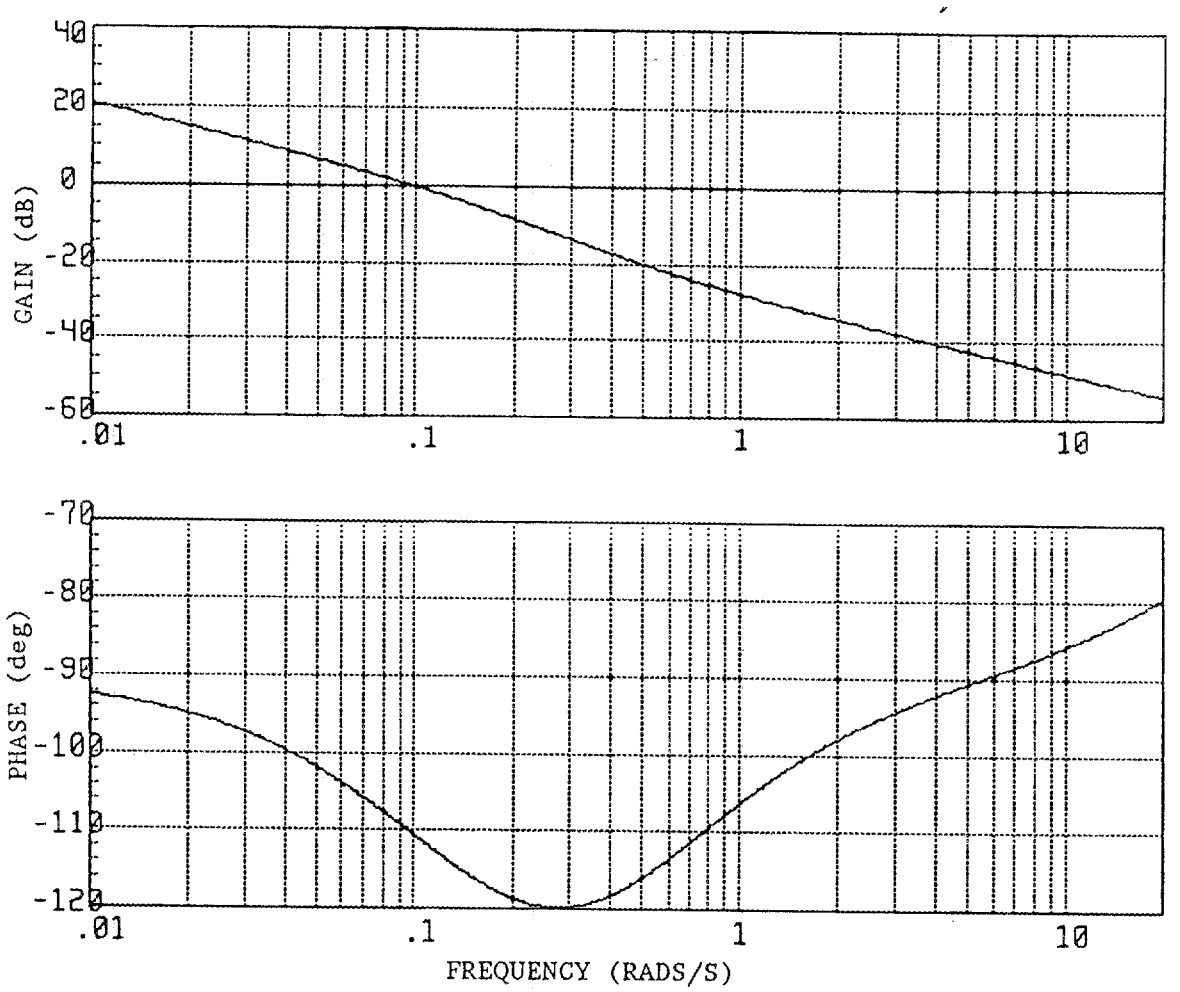

Fig. B7. Open-loop frequency response of PI control system.

APPENDIX C

Appendix C

CONCEPTS OF EIGENVECTORS, VECTOR NORMS, MATRIX NORMS AND SINGULAR VALUES

Eigenvalues and Eigenvectors

Assume that the linear time invariant (LTI) system is defined as

$$\dot{x} = Ax + Bu \tag{C1}$$

and

$$y = Cx \quad , \tag{C2}$$

where $x \epsilon R^r$, $u \epsilon R^p$, and $y \epsilon R^p$.

The eigenvalues of A are defined as $\lambda_i (i = 1,2,\ldots,n)$. The left eigenvector v_i^T of A is defined such that is satisfies

$$v_i^T(A - \lambda_i I) = 0 \quad , \tag{C3}$$

and the right eigenvector u_i of A is defined to satisfy

$$(A - \lambda_i I)u_i = 0 \quad . \tag{C4}$$

Note that for each left or right eigenvector there corresponds an eigenvalue λ_i which is already defined prior to the solution of the eigenvector. A characteristic of the left and right eignevectors is the orthogonal relationship that exists between them. The orthogonality relationship is defined as

$$v_i^T u_i = \begin{matrix} 1 & \text{for } i = j \\ 0 & \text{for } i \neq j \end{matrix} \tag{C5}$$

Considering that the A matrix has distinct eigenvalues, A can be decomposed as follows

$$A = T \Lambda T^{-1} \quad , \tag{C6}$$

where Λ is a diagonal matrix containing the eigenvalues, $T = [u_1, u_2, u_3, \ldots, u_n]$, and $T^{-1} = [v_1^T, v_2^T, v_3^T, \ldots, v_n^T]^T$. The representation of A given in Eq. C6 is called the eigenvector decomposition.[1,2]

Vector Norms

The size of a vector x is described by the concept of norm which most engineers tend to associate with length. Before the concept of vector norm is formally defined, let us review the concept of inner product. The inner product of the complex vectors $x = [x_1, x_2, \ldots, x_n]^T$ and $y = [y_1, y_2, \ldots, y_n]^T$ is defined as

$$\langle x,y \rangle = (x)^H y = x_1^* y_1 + x_x^* y_2 + \ldots + x_1^* y_n = \langle y,x \rangle \tag{C7}$$

where $(\ )^H$ indicates the hermitian transpose and $(\ )^*$ defines the complex conjugate. The hermitian transpose is defined as the complex conjugate transpose of the indicated vector or matrix.

The definition of the 1, 2 (Euclidean norm), ∞ vector norms are defined respectively as

$$\|x\|_1 = |x_1| + |x_2| + \ldots + |x_n| \tag{C8}$$

$$\|x\|_2 = (\langle x, x\rangle)^{1/2} = (x_1^* x_1 + x_2^* x_2 + \ldots + x_n^* x_n)^{1/2} \tag{C9}$$

$$\|x\|_\infty = \max_i |x_i| . \tag{C10}$$

Matrix Norms and Singular Values

Now the matrix norms of $\|A\|_1$, $\|A\|_2$, and $\|A\|_\infty$ will be defined for the $m \times n$ matrix A. The matrix A defines a linear transformation from the vector space V, called the domain to a vector space W called the range. Thus the linear transformation

$$A(x) = Ax \tag{C11}$$

transforms a vector x in $V \epsilon C^n$ into a vector $A(x)$ in $W \epsilon C^m$. The matrix norms of $\|A\|_1$, $\|A\|_2$, and $\|A\|_\infty$ are respectively defined as

$$\|A\|_1 = \max_{x \neq 0} \left(\frac{\|Ax\|_1}{\|x\|_1} \right) \tag{C12}$$

$$\|A\|_2 = \max_{x \neq 0} \left(\frac{\|Ax\|_2}{\|x\|_2} \right) = \ell_2 \text{norm} \tag{C13}$$

$$\|A\|_\infty = \max_{x \neq 0} \left(\frac{\|Ax\|_\infty}{\|x\|_\infty} \right) \tag{C14}$$

Since the ℓ_2 norm is a useful tool in control system analysis, further insight to its definition will now be given. The ℓ_2 norm of C13 can be written as

$$\|A\|_2 = \max_i (\lambda_i(A^H A))^{1/2}, \ i = 1,2,\ldots,n \tag{C15}$$

$$= \max_i (\lambda_i(AA^H))^{1/2}, \ i = 1,2,\ldots,n \quad . \tag{C16}$$

The matrices $A^H A$ and AA^H are hermitian and positive semidefinite. The eigenvalues of these matrices are real and non-negative.

Not let us define the singular value of a complex matrice $A \epsilon C^{nxn}$:

$$\sigma_i(A) = (\lambda_i(A^H A))^{1/2} = (\lambda_i(AA^H))^{1/2} \geq 0, \ i = 1,2,\ldots,n \quad . \tag{C17}$$

If $A \epsilon C^{mxn}$, which indicates that A is a nonsquare matrix, then

$$\sigma_i(A) = (\lambda_i(A^H A))^{1/2} = (\lambda_i(AA^H))^{1/2} \tag{C18}$$

for $1 \leq i \leq k$, where k = number of singular values = $min(m,n)$. The maximum and minimum singular values are defined respectively as

$$\sigma_{max}(A) = \|A\|_2 \tag{C19}$$

and

$$\sigma_{min}(A) = \max_{x = 0} \frac{\|Ax\|_2}{\|x\|_2} = \frac{1}{\|A^{-1}\|_2} , \tag{C20}$$

provided A is invertible.

The complex matrix A has the singular value decomposition as follows

$$A = U \Sigma V^H \tag{C21}$$

where

$$\Sigma = \begin{bmatrix} \sigma_1 & 0 & \dots & 0 \\ 0 & \sigma_2 & \dots & 0 \\ & & \dots & \sigma_n \\ 0 & 0 & \dots & 0 \\ 0 & 0 & \dots & 0 \end{bmatrix} \quad \text{is } m \times n$$

$$= \sigma_{ij} = 0 \text{ for } i \neq j \tag{21}$$

and U and V are respectively $m \times m$ and $n \times n$ unitary matrices. Also, it can be stated that

$$\Sigma = U^H A V. \tag{22}$$

The eigenvalues of

$$A^H A = V(\Sigma^H \Sigma) V^H \tag{23}$$

are σ_i^2, the diagonal elements of the diagonal matrix $\Sigma^H \Sigma$. The eigenvalues of

$$AA^H = U(\Sigma \Sigma^H) U^H \tag{24}$$

where $\Sigma \Sigma^H$ is diagonal and its elements σ_i^2 are the eigenvalues of AA^H.

APPENDIX C REFERENCES

1. G. H. Golub and C. F. Van Loan, Matrix Computations, John Hopkins University Press, Maryland, 1983.

2. B. Noble and J. W. Daniel, Applied Linear Algebra, Prentice-Hall, New Jersey, 1977.

INTERNAL DISTRIBUTION

1. J. L. Anderson
2. J. M. Bailey
3. S. J. Ball
4. R. E. Battle
5. R. C. Berkan
6. R. S. Booth
7. H. R. Brashear
8. C. R. Brittain
9. N. E. Clapp Jr.
10. B. G. Eads
11. C. E. Ford
12. D. N. Fry
13. J. M. Googe
14. W. R. Hamel
15. J. E. Jones Jr.
16-31. R. A. Kisner
32. H. E. Knee
33. R. C. Kryter
34. C. March-Leuba
35. J. March-Leuba
36. D. R. Miller
37. O. B. Morgan
38. J. K. Munro
39-58. G. V. Murphy
59. E. Newman, Jr.
60. L. C. Oakes
61. P. J. Otaduy
62. R. Perez
63. J. T. Robinson
64. L. Rovere
65. J. C. Schryver
66. R. E. Uhrig
67. B. R. Upadhyaya
68-73. J. D. White
74. T. L. Wilson
75. R. T. Wood
76. J. B. Ball (Advisor)
77. P. F. McCrea (Advisor)
78. ORNL Patent Section
79-80. Central Research Library
81. Y-12 Document Reference Section
82-83. Laboratory Records Department
84. Laboratory Records, ORNL-RC
85. ORNL Patent Office
86. I&C Publications Office

EXTERNAL DISTRIBUTION

87. Assistant Manager for Energy Research and Development, U.S. Department of Energy, Oak Ridge Operations Office, Oak Ridge, TN 37831.
88. A. D. Alley, General Electric Company, 6835 Via Del Oro Ave., P.O. Box 530954, San Jose, CA 95153-5354.
89. H. Alter, U.S. Department of Energy, NE53, Office of Breeder Reactor Technology Projects, Washington, DC 20545.
90. G. O. Beale, George Mason University, Electrical and Computer Engineering Dept., 4400 University Drive, Fairfax, VA 22030.
91. D. G. Carroll, General Electric Company, 6835 Via Del Oro Ave., P.O. Box 530954, San Jose, CA 95153-5354.
92. G. H. Chisholm, Experimental Breeder Reactor (EBR-II), P.O. Box 2528, Idaho Falls, ID 83401.
93. R. W. Colley, Electric Power Research Institute, 3412 Hillview Ave., P.O. Box 10412, Palo Alto, CA 94303.

94. W. L. Heckle, B&W Owners Group, ACS Task Force, c/o Duke Power Company, P.O. Box 33189, 422 South Church St., Charlotte, NC 28242.
95. J. H. Hopps, The Charles Stark Draper Laboratory, 555 Technology Square, Cambridge MA 02139.
96. M. Jamshidi, Dept. Electrical & Computer Engineering, Room 110, EECE Building, Albuquerque, NM, 87131.
97. E. Klevans, Dept. Nuclear Engineering, Pennsylvania State University, 231 Sackett Bldg., University Park, PA 16802.
98. L. R. Monson, EBR-II, P.O. Box 2528, Idaho Falls, ID 83401.
99. J. R. Penland, Science Applications, Inc., 1200 Prospect Street, P.O. Box 2351, La Jolla, CA 92038.
100. H. P. Planchon, Jr., Reactor and Plant Analysis, EBR-II Division, Argonne National Laboratory, 9700 South Cass Ave., Argonne, IL 60439.
101. G.V.S. Raju, Dept. Electrical & Computer Engineering, Ohio University, Athens, OH 45701.
102. J. Sackett, EBR-II, P.O. Box 2528, Idaho Falls, ID 83401.
103. S. E. Seeman, Hanford engineering Development Laboratory, P.O. Box 1970, Richland, WA 99352.
104. B. K. H. Sun, EPRI, Nuclear Power Division, 3412 Hillview Ave., P.O. Box 10412, Palo Alto, CA 94303.
105-163. Given distribution as shown in TID Category UC-530, Liquid Metal Fast Breeder Reactors: Base Technology.